

# MM-SpuBench: Towards Better Understanding of Spurious Biases in Multimodal LLMs

Wenqian Ye  
University of Virginia  
Charlottesville, VA, USA  
wenqian@virginia.edu

Bohan Liu  
University of Virginia  
Charlottesville, VA, USA  
qzp4ta@virginia.edu

Guangtao Zheng  
University of Virginia  
Charlottesville, VA, USA  
gz5hp@virginia.edu

Di Wang  
University of Virginia  
Charlottesville, VA, USA  
azm7tq@virginia.edu

Yunsheng Ma  
Purdue University  
West Lafayette, IN, USA  
yunsheng@purdue.edu

Xu Cao  
University of Illinois  
Urbana-Champaign  
Champaign, IL, USA  
xucao2@illinois.edu

Bolin Lai  
Georgia Institute of Technology  
Atlanta, GA, USA  
bolin.lai@gatech.edu

James M. Rehg  
University of Illinois  
Urbana-Champaign  
Champaign, IL, USA  
jrehg2@illinois.edu

Aidong Zhang  
University of Virginia  
Charlottesville, VA, USA  
aidong@virginia.edu

## Abstract

Spurious bias, a tendency to exploit spurious correlations between superficial input attributes and prediction targets, has revealed a severe robustness pitfall in classical machine learning problems. Multimodal Large Language Models (MLLMs), which leverage pre-trained vision and language models, have recently demonstrated strong capability in joint vision-language understanding. However, both the presence and severity of spurious biases in MLLMs remain poorly understood. In this work, we address this gap by analyzing the spurious biases in the multimodal setting and uncovering the specific inference-time data patterns that can manifest this problem. To support this analysis, we introduce MM-SPUBENCH, a comprehensive, human-verified benchmark dataset consisting of image-class pairs annotated with core and spurious attributes, grounded in our taxonomy of nine distinct types of spurious correlations. The benchmark is constructed using human-interpretable attribute information to capture a wide range of spurious patterns reflective of real-world knowledge. Leveraging this benchmark, we conduct a comprehensive evaluation of the state-of-the-art open-source and proprietary MLLMs with both standard accuracy and the proposed Conditional Generation Likelihood Advantage (CGLA). Our findings highlight the persistence of reliance on spurious correlations and the difficulty of mitigation on our benchmark. We hope this work can inspire new technical strides to mitigate these biases. Our benchmark is publicly available at <https://huggingface.co/datasets/mmbench/MM-SpuBench>.

## CCS Concepts

• **Computing methodologies** → **Scene understanding**.

## Keywords

Spurious Correlations, Multimodal LLMs, Dataset and Benchmark

### ACM Reference Format:

Wenqian Ye, Bohan Liu, Guangtao Zheng, Di Wang, Yunsheng Ma, Xu Cao, Bolin Lai, James M. Rehg, and Aidong Zhang. 2026. MM-SpuBench: Towards Better Understanding of Spurious Biases in Multimodal LLMs. In *Proceedings of the 32nd ACM SIGKDD Conference on Knowledge Discovery and Data Mining V.1 (KDD '26)*, August 09–13, 2026, Jeju Island, Republic of Korea. ACM, New York, NY, USA, 21 pages. <https://doi.org/10.1145/3770854.3785678>

## 1 Introduction

Recently, we have witnessed the rise of highly performant Large Language Models (LLMs) [14, 15, 19, 64, 69, 84] and Vision Foundation Models (VFM) [26, 51] powered by advancements in vision language modeling, as well as the availability of large-scale training data and substantial computational resources. Building on these advancements, multimodal Large Language Models (MLLMs) [2, 4, 18, 39, 43, 46, 62, 90] emerge as the new frontier of foundation models by integrating both LLMs and VFMs for joint visual and text understanding. MLLMs have demonstrated significant performance gains in visual reasoning tasks, such as image perception [32, 41], visual question answering [78], and instruction following [12].

Despite the impressive performance of MLLMs, the robustness of MLLMs remains largely under-explored. One critical robustness issue in deep learning models is the *spurious bias*, a tendency to exploit spurious correlations between superficial input attributes and prediction target [77] for higher in-distribution performance. For example, image classifiers tend to identify a waterbird by solely using the water background (*spurious attribute*) that frequently co-occurs with it in the training data, whereas the bird's intrinsic features (*core attributes*), such as color and shape, should be the true indicators for accurate predictions [22, 57]. Previous research



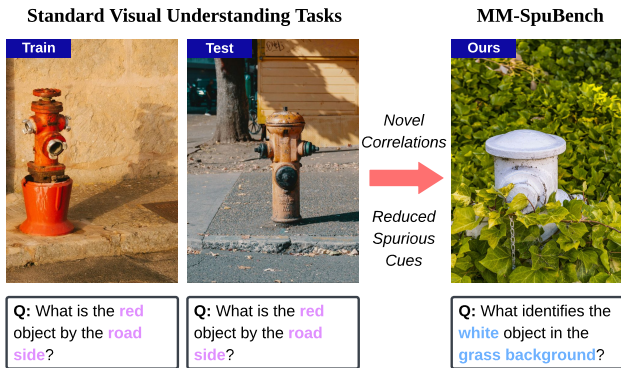


**Figure 1: Schematic illustration of standard visual understanding tasks and MM-SPUBENCH. In standard tasks, both training and testing data consist of spurious correlations, such as fire hydrants frequently co-occurring with red color and roadside. In MM-SPUBENCH, we introduce novel correlations by reducing spurious cues, such as fire hydrants paired with white color and grass background.**

works have primarily defined and mitigated spurious bias in single-modality classification tasks [35, 38, 48, 57, 86].

Getting back to MLLMs, their pre-trained vision and text encoders also tend to learn spurious correlations within their respective modalities [20, 24, 67, 74]. In the MLLM training for visual grounding, the ability to align specific visual regions with corresponding textual labels may be hindered by spurious correlations in both vision and language modalities. Consequently, at the inference stage, where the captured multi-modal spurious correlations break due to distribution shifts, MLLMs tend to make biased predictions. With the main object of the fire hydrant shown in Fig. 1, multi-modal spurious correlations in the training (i.e., fire hydrant and red color) no longer hold in the inference data (i.e., fire hydrant and white color), leading the model to select the wrong answer in the VQA inference data. We refer to the above phenomenon as *multimodal spurious bias*. Given the prevalence of spurious biases in classical machine learning problems, a natural question arises:

Do MLLMs also exhibit spurious biases?  
If so, to what extent are they affected?

In this paper, we formally define the concept of *multimodal spurious bias* that involves the spurious correlations within multiple modalities. Our definition begins with the notion of an *anchor*, an abstract, semantically meaningful concept that is central to a VQA task and is grounded in both modalities. For example, the anchor for the VQA from the training data in Fig. 1 is the concept of fire hydrant, and it exists in both the image and the text. The introduction of *anchor* allows us to define spurious correlations within vision and language modalities conveniently. There are spurious correlations between visual features “fire hydrant” and “roadside” and the spurious correlation between text “fire hydrant” and “red” or “road”, as shown in Fig. 1. These correlations occur frequently in the training data and when such correlations break (i.e., with whi te

color and grass background), the MLLMs will lead to failures in prediction.

To better study and quantify the multimodal spurious bias, it is essential to construct dedicated evaluation data that targets robustness failures in MLLMs. To address this need, we propose MM-SPUBENCH, a comprehensive VQA benchmark with nine categories of spurious correlations specifically designed to evaluate the reliance of MLLMs on instance-level spurious correlations learned during training. To curate the dataset, we introduce a simple yet effective semiautomatic pipeline that leverages parametric knowledge [2] to extract and annotate attributes of inference data. We carefully select 10,773 image samples from five open-source datasets, design 2,400 VQA questions containing derived core/spurious attributes, and categorize spurious biases into 9 categories, shown in Fig. 2. We then propose both Standard VQA Accuracy within the nine categories and a novel Conditional Generation Likelihood Advantage (CGLA) on MM-SPUBENCH as metrics for evaluating fine-grained spurious biases. CGLA measures the impact of these attributes on the output token distributions of MLLMs. These two evaluation metrics complement each other by providing *structured* and *unstructured* evaluation setups and offer both top-down and bottom-up studies on examining spurious correlations in MLLMs. With the novel correlations and reduced spurious correlations in our benchmark, models rely minimally on learned spurious correlations. Therefore, their tendency towards spurious biases can be measured quantitatively.

**Our contributions are summarized as follows:** (1). We formally define multimodal spurious bias in MLLMs, highlighting how spurious correlations can compromise robustness and lead to failures in current MLLMs. (2). We propose MM-SPUBENCH, a novel benchmark featuring 10,773 realistic images with concept-based attribute information, paired with a set of 2,400 VQA data, designed to systematically evaluate current MLLMs across 9 distinct categories of spurious biases. (3). We conduct an in-depth analysis of current representative MLLMs with two proposed metrics and perform experiments on various prompting techniques to mitigate spurious biases. The results reveal some current limitations and shed light on future research directions.

## 2 Related Works

*Robustness in multimodal LLMs.* Recent proprietary MLLMs, such as GPT-4V [2], Claude [4], and Gemini [62], have demonstrated notable robustness to various distribution shifts, showcasing the potential in handling diverse and challenging real-world scenarios. Moreover, thanks to the high-quality visual instruction tuning data, we have seen improved robustness [63] in open-source models like InternVL3 [90], Llama-3.2-Vision [46], and LLaVA [39]. Nevertheless, MLLMs still face challenges in handling visually complex images with spurious correlations, which cause hallucinations and non-trustworthy behaviors [21, 25], exposing the limitations in visual search mechanisms [9, 70] and visual grounding capabilities [56, 63, 82]. Our paper focuses on the fundamental spurious bias issue in the multimodal setting, as it reflects a broad family of biases prevalent in current MLLMs.

 <b>Background</b>	 <b>Texture and Noise</b>	 <b>Co-occurring Objects</b>
<p><b>Question:</b> Which feature best indicates the identity of the object placed on the bed?</p> <p><b>Choices:</b></p> <ul style="list-style-type: none"> <li>A. The pillow nearby</li> <li>B. The wooden furniture</li> <li>C. The object's metal material</li> <li>D. The patterned bedspread</li> </ul>  <p><b>Core Attributes:</b> rectangular shape, metal material, slight lip  <b>Spurious Attributes:</b> on a bed, near a pillow, patterned bedspread, wooden furniture  <b>Difficulty:</b> Easy</p>	<p><b>Question:</b> Which feature best indicates the identity of the object with sketchy lines and abstract representation?</p> <p><b>Choices:</b></p> <ul style="list-style-type: none"> <li>A. Terrier shape</li> <li>B. Toy characteristics</li> <li>C. Papillon traits</li> <li>D. Entertainment center</li> </ul>  <p><b>Core Attributes:</b> distinct face, furry texture, terrier shape  <b>Spurious Attributes:</b> sketch style, abstract lines, drawing orientation  <b>Difficulty:</b> Medium</p>	<p><b>Question:</b> Which feature best indicates the identity of the object on the surface?</p> <p><b>Choices:</b></p> <ul style="list-style-type: none"> <li>A. Kitchen counter</li> <li>B. Cutting boards</li> <li>C. Kitchen appliances</li> <li>D. The object's laces</li> </ul>  <p><b>Core Attributes:</b> shoe shape, laces, sole  <b>Spurious Attributes:</b> kitchen counter, cutting boards, kitchen appliances, utensil holder  <b>Difficulty:</b> Medium</p>
 <b>Relative Size</b>	 <b>Colorization</b>	 <b>Orientation</b>
<p><b>Question:</b> Which feature best indicates the identity of the object near the bottle?</p> <p><b>Choices:</b></p> <ul style="list-style-type: none"> <li>A. Its small size</li> <li>B. Its cylindrical shape</li> <li>C. The lace tablecloth</li> <li>D. The nearby bottle</li> </ul>  <p><b>Core Attributes:</b> cylindrical shape, plastic material, fits in bottle  <b>Spurious Attributes:</b> small size, near bottle, transparent  <b>Difficulty:</b> Hard</p>	<p><b>Question:</b> Which feature best indicates the identity of the object near the dish rack?</p> <p><b>Choices:</b></p> <ul style="list-style-type: none"> <li>A. The pink color</li> <li>B. The bottle shape</li> <li>C. The squeeze cap</li> <li>D. The liquid inside</li> </ul>  <p><b>Core Attributes:</b> squeeze bottle, soap inside  <b>Spurious Attributes:</b> bottle shape, pink color, squeeze cap, dish rack  <b>Difficulty:</b> Medium</p>	<p><b>Question:</b> Which feature best indicates the identity of the object being held near the kitchen sink?</p> <p><b>Choices:</b></p> <ul style="list-style-type: none"> <li>A. The kitchen sink</li> <li>B. The blurry image</li> <li>C. The object's label</li> <li>D. The hand holding it</li> </ul>  <p><b>Core Attributes:</b> transparent container, cylindrical shape, liquid content  <b>Spurious Attributes:</b> kitchen sink, held in hand, blurry image, upside down  <b>Difficulty:</b> Hard</p>
 <b>Lighting and Shadows</b>	 <b>Perspective and Angle</b>	 <b>Shape</b>
<p><b>Question:</b> Which feature best indicates the identity of the object that is laid out on the floor?</p> <p><b>Choices:</b></p> <ul style="list-style-type: none"> <li>A. The hanger</li> <li>B. The position on floor</li> <li>C. The shadow</li> <li>D. The fabric</li> </ul>  <p><b>Core Attributes:</b> overall shape, fabric, bodice, skirt  <b>Spurious Attributes:</b> shadows, lighting, position on floor, nearby objects  <b>Difficulty:</b> Medium</p>	<p><b>Question:</b> Which feature best indicates the identity of the small, gold-colored object?</p> <p><b>Choices:</b></p> <ul style="list-style-type: none"> <li>A. The gold color</li> <li>B. The object's circular shape</li> <li>C. The object's central hole</li> <li>D. The textured background</li> </ul>  <p><b>Core Attributes:</b> central hole, flat structure, small size, circular shape, sewing loop  <b>Spurious Attributes:</b> textured background, gold color, side view, circular shape, small object  <b>Difficulty:</b> Hard</p>	<p><b>Question:</b> Which feature best indicates the identity of the object with an elongated shape?</p> <p><b>Choices:</b></p> <ul style="list-style-type: none"> <li>A. Smooth surface</li> <li>B. Sharp blade</li> <li>C. Jigsaw structure</li> <li>D. The handle</li> </ul>  <p><b>Core Attributes:</b> blade-like structure, handle, elongated shape, jigsaw blade  <b>Spurious Attributes:</b> smooth surface, dark background, sheen  <b>Difficulty:</b> Hard</p>

Figure 2: Samples from each spurious correlation type in MM-SpuBENCH. The images and questions require human-level cognitive abilities to judge the core information in the provided choices.

*Spurious attribute detection.* Spurious attributes can negatively impact a model’s generalization capabilities [22, 79] and are commonly used to reveal the model’s robustness pitfalls. Some previous studies predefine [42, 54, 71] a list of spurious attributes relevant to the task, which also refer to group labels. However, such labels require domain knowledge [16, 49] and extensive human annotation efforts [50, 83]. For example, object backgrounds [72] and image textures [23] have been identified as spurious attributes that can bias the predictions of deep learning models. Recent research has employed explainable data generation methods [1, 52] to detect or exploit spurious biases in LLMs [30, 53, 76, 87]. In our work, we use the LLM’s parametric knowledge to parse the information in ground truth labels and incorrectly predicted labels by state-of-the-art vision encoders for spurious concepts that are human-understandable. These concepts are used to build challenging VQA tasks for benchmarking MLLMs.

*Benchmarks on multimodal LLMs.* In classical machine learning problems, there have been several benchmarks [57, 85] to evaluate spurious correlations on classification tasks. In the multimodal setting, previous benchmarks such as TextVQA [60] and GQA [33] have focused on traditional VQA queries. More recently, works such as MM-Vet [80], POPE [36], and MM-Bench [40] have been developed to specifically evaluate multimodal LLMs in terms of hallucination, reasoning, and robustness. These evaluations have uncovered that multimodal LLMs can suffer from hallucination [8, 13, 31], catastrophic forgetting [81, 89], and a lack of robustness [11, 17, 68]. Unlike previous VQA benchmarks, which only include question-answer data, our benchmark also incorporates concept-based information on both core and spurious attributes. This addition helps researchers distinguish between core and spurious information, thereby facilitating the future development of spurious bias mitigation methods.

### 3 Spurious Biases in Multimodal LLMs

#### 3.1 Preliminary

We consider a typical multimodal setting involving a vision modality  $\mathcal{X}$  and a language modality  $\mathcal{Y}$ . We introduce an abstract concept *anchor*  $a$  for each image-text encoding pair  $(\mathbf{x}, \mathbf{y})$ , representing the primary entity or object that forms the central focus. Given an image input  $\mathbf{x} \in \mathcal{X}$  and a text input  $\mathbf{y} \in \mathcal{Y}$ , an MLLM algorithm learns a mapping function  $\phi : \mathcal{X} \times \mathcal{Y} \rightarrow \mathcal{C}$ , such that the response  $c = \phi(\mathbf{x}, \mathbf{y}|a)$ , where  $c \in \mathcal{C} \subset \mathcal{Y}$  is generated autoregressively based on the image  $\mathbf{x}$  and text context  $\mathbf{y}$ . In the VQA setting, the *anchor* label  $a$  is a latent variable. The generated response  $c$  is expected to correlate with the core information related to this *anchor*.

To analyze spurious biases in MLLMs, without loss of generality, we assume that each input from both modalities contains core features, spurious features, and noise features, following prior works [47, 57, 58, 73]. Specifically, we represent the vision input as  $\mathbf{x} = [x_{\text{core}}, x_{\text{spu}}, x_{\text{noise}}]$  and the language input as  $\mathbf{y} = [y_{\text{core}}, y_{\text{spu}}, y_{\text{noise}}]$ . In both modalities, the core features  $(x_{\text{core}}, y_{\text{core}})$  are essential for generating the intended response  $c$ . Spurious features  $(x_{\text{spu}}, y_{\text{spu}})$  are non-essential to  $c$  but may exhibit statistical correlations with it, while noise features  $(x_{\text{noise}}, y_{\text{noise}})$  capture sample-specific details, which represent some minor independent perturbations in images or irrelevant contexts in texts.

#### 3.2 From Single Modality to Multi-modality

We start with the analysis of single-modality spurious bias. Without loss of generality, we first consider the vision modality  $\mathcal{X}$ . Assume there exists a data pair  $(\mathbf{x}, c)$ , with  $\mathbf{x}$  as the vision input and  $c$  as the true output, derived from a training dataset, and  $\mathbf{z}$  is a spurious attribute of  $\mathbf{x}$ . Given that  $\mathbf{z}$  and  $c$  form a spurious correlation in the training set, the condition for a model to develop spurious bias is as follows:  $p_{\text{train}}(\mathbf{z}|c, x_{\text{core}}) \gg p_{\text{train}}(\mathbf{z}|x_{\text{core}})$  [75], which means that the probability of  $\mathbf{z}$  given  $c$  and the core feature  $x_{\text{core}}$  is much higher than the probability of  $\mathbf{z}$  given only the core feature  $x_{\text{core}}$ . Similarly, in the language modality, given a data pair  $(\mathbf{y}, c)$  and the associated spurious attribute  $\mathbf{z}$ , the condition for developing spurious bias in the language modality can be expressed as:  $p_{\text{train}}(\mathbf{z}|c, y_{\text{core}}) \gg p_{\text{train}}(\mathbf{z}|y_{\text{core}})$ . We extend our analysis to the multimodal setting and define multimodal spurious bias as follows.

**Definition 3.1** (Multimodal Spurious Bias). Given an input image  $\mathbf{x} = [x_{\text{core}}, x_{\text{spu}}, x_{\text{noise}}]$ , a text input  $\mathbf{y} = [y_{\text{core}}, y_{\text{spu}}, y_{\text{noise}}]$ , the desired response  $c$  to the joint inputs  $\mathbf{x}$  and  $\mathbf{y}$ , and a spurious attribute  $\mathbf{z}$  shared by  $x_{\text{spu}}$  and  $y_{\text{spu}}$ , the spurious correlations in the multimodal setting can be expressed as follows:

$$p(\mathbf{z}|x_{\text{core}}, y_{\text{core}}, c) \gg p(\mathbf{z}|x_{\text{core}}, y_{\text{core}}). \quad (1)$$

Under this condition, an MLLM tends to develop spurious multimodal bias, which is the tendency to use the spurious correlations between spurious attributes  $\mathbf{z}$  and the desired responses  $c$  to generate responses given the core features in both modalities. Detailed discussions on the definition are provided in the Appendix.

#### 3.3 How to Reveal Multimodal Spurious Bias

In principle, revealing spurious biases in models requires the construction of a test set in which the spurious correlations are distributionally shifted relative to those in the training data. For example,

in the vision modality, a common approach [57] is to curate a test set where the spurious correlation between a spurious attribute  $\mathbf{z}$  and a target  $c$  becomes  $p_{\text{test}}(\mathbf{z}|c, x_{\text{core}}) = p_{\text{test}}(\mathbf{z}|x_{\text{core}})$ , compared to  $p_{\text{train}}(\mathbf{z}|c, x_{\text{core}}) \gg p_{\text{train}}(\mathbf{z}|x_{\text{core}})$  in the training set. Thus, the correlation between  $\mathbf{z}$  and  $c$  only holds in the training data and no longer holds in the test data. Motivated by this, we propose the following multimodal data generation method to reveal multimodal spurious bias.

We first select images with the spurious attribute  $\mathbf{z}$  following  $p_{\text{test}}(\mathbf{z}|c, x_{\text{core}}) \approx p_{\text{test}}(\mathbf{z}|x_{\text{core}})$  in the vision modality. This can be approximated by collecting misclassified samples whose spurious attributes are unlikely to correlate with certain labels, as seen in the training data. Given the anchor (true label), we derive the core and spurious attributes from the misclassified samples. Based on the derived attributes, we create individual VQA tasks that contain various spurious textual attributes. This process simulates  $p_{\text{test}}(\mathbf{z}|c, y_{\text{core}}) \approx p_{\text{test}}(\mathbf{z}|y_{\text{core}})$ . In this way, the spurious correlation learned by the model between  $c$  and  $\mathbf{z}$  is broken, thus causing failure if the models rely on spurious correlations for prediction.

However, constructing such a test set requires knowing  $\mathbf{z}$  *a priori*, which is challenging in the multimodal scenario where only core objects are annotated in previous datasets. We address this challenge by proposing a semi-automatic curation method and producing a comprehensive human-verified VQA benchmark. We explain our curation pipeline with details in Section 4.2.

## 4 MM-SPUBENCH: The Benchmark for Multimodal Spurious Biases

### 4.1 Types of Spurious Correlations

We first define nine types of spurious correlations to comprehensively cover the spurious correlations in real-world data, as shown in Fig. 2. Although some research [21] exists with similar definitions, such as shape bias and texture bias, we are interested in diverse types of spurious correlations between attributes and core objects in images rather than focusing on a single type of bias.

### 4.2 Construction of MM-SPUBENCH

In this section, we demonstrate the three steps for the construction of MM-SPUBENCH as shown in Fig. 3.

*Image pre-selection.* As shown in Fig. 3 (left), we pre-select images with their class labels from various image classification datasets to ensure the diversity of our benchmark. ObjectNet [10] serves as our primary image source due to its numerous observable spurious biases. To supplement this dataset, we collect data from descendants of ImageNet-Hard [61] that focus on domain generalization evaluation, including ImageNet-R (rendition) [27], ImageNet-Sketch [66], ImageNet-A [29], and ImageNet-C [28]. They complement categories of spurious biases not present in ObjectNet, such as texture/noise and relative size. We choose existing datasets rather than using parametric image generation techniques [25] to ensure our benchmark reflects realistic spurious biases found in the real world, avoiding additional biases that could render the benchmark results unrepresentative. See Appendix for the dataset details.

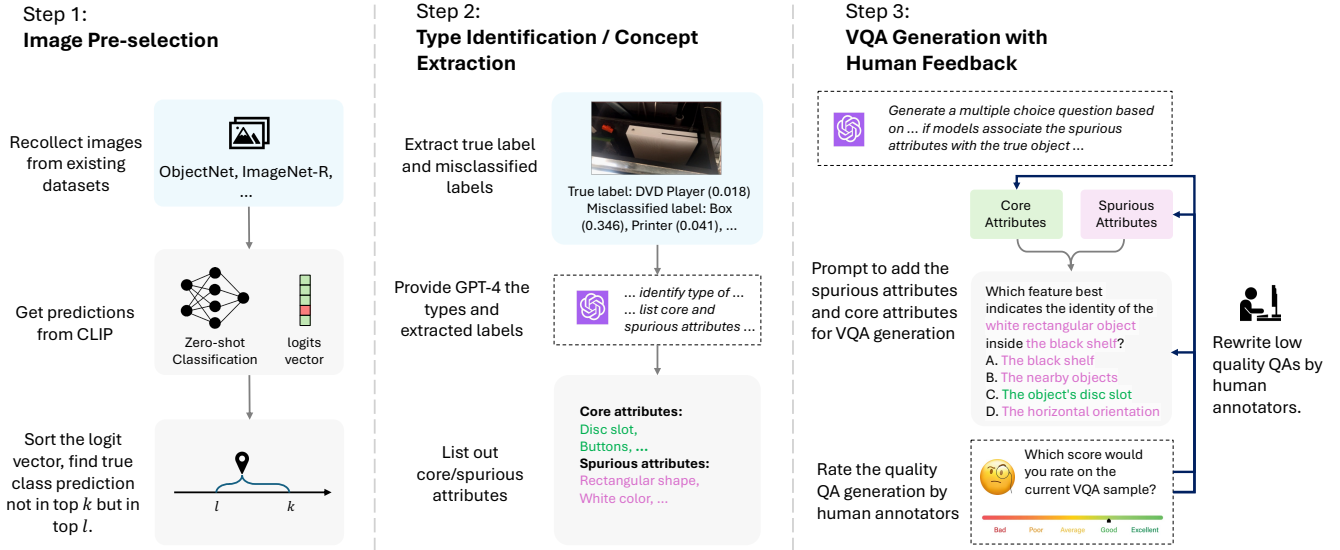


**Figure 3: Construction of the MM-SpuBENCH.** Left: Pre-select images where CLIP’s true class prediction is not in the top  $k$  but is in the top  $l$ . Middle: Identify spurious correlations and list core/spurious attributes. Right: Generate multiple-choice questions based on the spurious bias type and core/spurious attributes with human supervision.

To select image data with potential spurious attributes, we use the most commonly employed vision encoder in current open-source MLLMs, CLIP-ViT-L/14@336px [55], for zero-shot classification. As evidenced by [63, 74], CLIP models significantly suffer from the spurious correlations learned during pretraining. We utilize the logit vectors from the classification output to find samples where CLIP’s true class prediction is in the range of top- $k$  and top- $l$ , where  $k$  and  $l$  are hyperparameters to control whether the misclassification is due to spurious biases rather than annotation noise or insufficient visual cues. For each image, we record the ground truth class and top misclassified classes. Some pairs of ground truth labels and misclassified labels indicate the spurious correlations the vision encoder relies on during the training process, guiding the following design of our benchmark. For image pre-selection, we deploy  $k = 3, l = 20$  for ObjectNet and  $k = 3, l = 40$  for ImageNet-Hard. With this selection strategy, we curate a dataset with a total of 10,773 image samples with labels. To retrieve a high-quality VQA subset, we deploy  $k = 5, l = 10$  for ObjectNet and  $k = 3, l = 40$  for ImageNet-Hard with a total of 2,400 image/label samples.

*Type identification and attribute extraction.* In Fig. 3 (middle), we leverage images along with their corresponding ground truth and misclassified labels to identify the types of spurious biases and understand their underlying causes. To achieve this, we employ a strong LLM (i.e., GPT-4o) as a concept generator, utilizing the chain-of-thought strategy to extract detailed and useful concept-based information from both the ground truth and misclassified labels. For each image, we generate two types of attributes: core and spurious attributes. Core attributes are generated based on the ground truth label. They describe the intrinsic properties of the core object within the image, such as shape, color, and specific distinguishable features inherent to the object. Spurious attributes are generated based on the misclassified labels. These attributes

**Table 1: Main statistics of MM-SpuBENCH.** Each image may contain at most two types of spurious correlations.

Statistic	Value
Total instances	2,400
Background (BG)	1,908 (79.50%)
Texture and Noise (TN)	288 (12.00%)
Co-occurring Objects (CO)	903 (37.62%)
Relative Size (RS)	75 (3.12%)
Colorization (Col.)	248 (10.33%)
Orientation (Ori.)	764 (31.83%)
Lighting and Shadows (LS)	103 (4.29%)
Perspective and Angle (PA)	100 (4.17%)
Shape (Sha.)	401 (16.71%)

do not have direct correlations with the primary object but still influence the model’s inference process, leading to spurious biases. To maintain a balanced and fair evaluation in our VQA benchmark, we limit the number of both core and spurious attributes to 5 per image, ensuring consistent evaluation and fair comparison across the dataset. Then we used the derived attributes together with the image to let the LLM determine the types of spurious biases (at most 2) in the image. We present the type distribution in our dataset in Table 1.

*Visual Question Answering (VQA) curation.* In Fig. 3 (right), we build upon the identified core and spurious attributes to create VQA pairs that evaluate a model’s robustness to multimodal spurious biases. To reduce crowdsourcing, we adopt a semiautomatic improvement process for VQA curation. Using selected images and their core/spurious attributes, we design prompts that incorporate spurious attributes into the questions and use core attributes to

generate one correct option referring to the anchor. A strong LLM uses this information to produce multiple-choice questions to test whether a model can identify the golden response in the presence of spurious attributes. These questions avoid direct cues to the core attributes or true labels, instead describing the core object with its spurious attributes and spatial position. Each question randomly incorporates the derived core and spurious attributes from the previous step, with only one ground truth answer and three misleading options. Following the data generation, five human annotators review and rate QA triplets on a scale of 1 to 5. Based on this feedback, annotators revise the core/spurious attributes, QA pairs, and ground truth answers with human-grounded knowledge. An overview of the MM-SPUBENCH data is illustrated in Fig. 2.

### 4.3 Beyond VQA: Conditional Generation Likelihood

The standard VQA accuracies on our dataset provide high-level insight into the robustness of the MLLMs against spurious biases. To benchmark MLLMs at a finer level, with less dependency on the MLLMs’ overall instruction-following and visual recognition capabilities, we calculate the MLLMs’ preferences for all triplets of desired responses, textual attributes, and visual inputs. Inspired by McMilin [44] on using single-token distribution to investigate correlations in Pretrained Bidirectional Language Models, we adopt the generation probability as a lens to reveal the learned correlations of MLLMs.

We extend the single-token generation probability to MLLMs and adapt for causal generation as follows: with MLLMs that consider visual representations as a pretext to the generation, the probability of the next token is  $P(s_i | \mathbf{s}_{i-1}, \mathbf{v})$ , where  $s_i$  is the current generated token,  $\mathbf{s}_{i-1}$  is all text tokens before position  $i$  and  $\mathbf{v}$  is a vector of visual features. For a fixed textual sequence  $\mathbf{o} := o_0, o_1, \dots, o_k$ , we compute the logarithmic likelihood of text generation in the model from a pretext pair  $(\mathbf{s}_{i-1}, \mathbf{v})$ :

$$\text{MLLM}(\mathbf{o} | \mathbf{s}_{i-1}, \mathbf{v}) = \prod_{i=l}^{l+k} P(s_i = o_i | \mathbf{s}_{i-1}, \mathbf{v}) \quad (2)$$

At inference time, we formulate a generation prompt, consisting of a system prompt, a user prompt, and an assistant prefix, as input for the generation of MLLM. Denote  $g(\cdot)$  as the prompt function that takes an input attribute and produces a natural text sequence containing the input attribute. The Conditional Generation Likelihood under an input attribute text  $\mathbf{t}$  of the caption of the ground truth label as the true response  $\mathbf{c}$  is

$$\text{CGL}(\mathbf{c} | \mathbf{t}, \mathbf{v}) = \log[\text{MLLM}(\mathbf{c} | g(\mathbf{t}), \mathbf{v})] \quad (3)$$

We propose Conditional Generation Likelihood Advantage (CGLA) as a metric to detect the learned spurious bias of an MLLM. We calculate the Conditional Generation Likelihood following Equation 3. Then, CGLA of the true response  $\mathbf{c}$  of one attribute text  $\mathbf{t}_1$  over another attribute text  $\mathbf{t}_2$  is calculated by subtracting  $\text{CGL}(\mathbf{c}, \mathbf{t}_2)$  from  $\text{CGL}(\mathbf{c}, \mathbf{t}_1)$ , which is defined as follows:

$$\text{CGLA}(\mathbf{c} | \mathbf{t}_1; \mathbf{t}_2, \mathbf{v}) = \text{CGL}(\mathbf{c} | \mathbf{t}_1, \mathbf{v}) - \text{CGL}(\mathbf{c} | \mathbf{t}_2, \mathbf{v}) \quad (4)$$

In our experiments, given an annotated set of spurious and core attributes, denoting  $\mathbf{t}_{\text{core}}$  as the core attribute,  $\mathbf{t}_{\text{spu}}$  as a spurious attribute and  $\mathcal{T}_{\text{spu}}$  as the set of spurious attributes, we consider

the CGLA difference between the core attribute and the spurious attribute that makes generating the object class most probable as a measurement of the model’s preference toward spurious attributes as a condition for the corresponding object class. We specifically select the spurious attribute that maximizes the generation probability because it represents the most tempting shortcut available to the model, allowing our metric to quantify the model’s bias under a worst-case condition, providing a stringent test of its robustness. We formally define it as follows:

$$\text{CGLA}_{\min}(\mathbf{c} | \mathbf{t}_{\text{core}}; \mathcal{T}_{\text{spu}}, \mathbf{v}) = \min_{\mathbf{t}_{\text{spu}} \in \mathcal{T}_{\text{spu}}} (\text{CGLA}(\mathbf{c} | \mathbf{t}_{\text{core}}; \mathbf{t}_{\text{spu}}, \mathbf{v})) \quad (5)$$

Based on the causal language modeling objective of MLLMs, CGLA measures the likelihood difference between attributes as conditions for generating a particular text sequence as output. Under our evaluation setup, a positive  $\text{CGLA}_{\min}$  means that the core attribute is the most competitive condition for generating the object label among the spurious attributes, and a negative  $\text{CGLA}_{\min}$  means that at least one spurious attribute is a better condition for generating the object label. Therefore, we apply the unit step function to  $\text{CGLA}_{\min}$ . When averaged over the dataset, this metric measures an MLLM’s accuracy in modeling the correct condition-anchor relationship under our generative evaluation setting. Given the unit step function  $\mathbb{1}(\cdot)$ , the generative accuracy  $\text{CGLA}_{\text{acc}}$  is defined:

$$\text{CGLA}_{\text{acc}}(\mathbf{c} | \mathbf{t}_{\text{core}}; \mathcal{T}_{\text{spu}}, \mathbf{v}) = \mathbb{1}(\text{CGLA}_{\min}(\mathbf{c} | \mathbf{t}_{\text{core}}; \mathcal{T}_{\text{spu}}, \mathbf{v})) \quad (6)$$

## 5 Results and Analysis

### 5.1 Baselines

For proprietary MLLMs, we chose Gemini 1.5 Pro [62], GPT-4V/GPT-4o [2], and the Claude 3 family models (Haiku, Sonnet, Opus)[4], which are the mainstream MLLMs. The input for these models consists of a system prompt and a format prompt that describes the task and the question with four options, while the expected output includes the predicted option and an explanation to help us understand the reasoning processes. For open-source MLLMs, following previous works [40, 63], we select current state-of-the-art models that excel in general VQA tasks, including InternVL3 [90], Llama3.2 [46], LLaVA [39], and Qwen-VL [6, 7], with variants of LLM backbones. The input for these models includes a system prompt that describes the task and the question with four options, with the expected output being only the option following a vanilla multiple-choice VQA setup.

### 5.2 Experimental Details

*Standard VQA Experiment.* To ensure fair comparisons, we shuffle the answer choices for each question to eliminate option biases across MLLM models. For open-source models, all inference experiments are run on NVIDIA A100 and A6000 GPUs. Each experiment is repeated with three different random seeds, and the reported values are the average of these runs. For consistency and reproducibility, we perform *greedy sampling*. Due to variations in the capabilities of each model, we design separate prompts to ensure the models can output the correct format of choice from our benchmark. To assess the MLLMs’ performances on MM-SPUBENCH, we use accuracy as the metric to determine MLLMs’ robustness to spurious biases. For proprietary models, we only include cases when

**Table 2: Zero-shot results of MLLMs on MM-SPUBENCH. All numbers are percentage accuracies. Green color indicates higher accuracy, and red color indicates lower accuracy. The dashes indicate that the proprietary models’ backbones are not applicable.**

MLLM	LLM Backbone	MM-SPUBENCH									Average
		BG	TN	CO	RS	Co1.	Ori.	LS	PA	Sha.	
Gemini 1.5 Pro [62]	—	60.12	55.35	63.46	50.28	53.25	62.86	60.38	48.15	54.79	58.06
Claude 3 Haiku [4]	—	55.45	53.77	57.12	40.22	45.12	55.71	47.17	37.04	39.85	52.06
Claude 3 Sonnet [4]	—	78.06	76.57	81.35	61.45	65.85	81.43	75.47	59.26	60.92	74.82
Claude 3 Opus [4]	—	80.43	76.10	83.65	64.80	66.67	82.86	83.02	70.37	67.82	77.18
GPT-4V [2]	—	83.58	82.39	85.33	67.60	72.65	81.43	84.91	70.37	73.36	80.90
GPT-4o [2]	—	80.64	81.13	83.85	60.89	69.39	80.00	83.02	65.43	67.18	77.97
InternVL3-8B [90]	Qwen2.5-7B [7]	74.48	70.87	78.01	58.87	60.42	73.79	70.67	68.00	67.33	71.92
InternVL3-14B [90]	Qwen2.5-14B [7]	81.55	80.51	82.85	64.92	66.32	75.73	80.00	69.00	64.09	77.92
InternVL3-38B [90]	Qwen2.5-32B [7]	86.11	83.28	88.22	73.79	70.14	85.44	81.33	76.00	74.56	83.04
Llama-3.2-VI-11B [46]	Llama-3.1-8B [45]	74.58	73.53	76.57	59.27	62.85	68.93	74.67	63.00	61.35	71.71
LLaVA-v1.5-7B [39]	Llama-2-7B [65]	41.19	41.31	39.53	33.47	34.38	40.78	38.67	38.00	35.16	39.54
LLaVA-v1.5-13B [39]	Llama-2-13B [65]	63.31	62.57	63.48	39.52	46.18	55.34	56.00	50.00	47.63	59.08
LLaVA-v1.6-mis-7B [39]	Mistral-7B [34]	39.83	39.20	40.71	32.26	38.54	38.83	41.33	42.00	33.67	38.88
LLaVA-v1.6-vic-13B [39]	Vicuna-13B [88]	24.53	26.25	24.74	20.97	23.96	28.16	24.00	19.00	23.44	24.58
LLaVA-v1.6-34B [39]	Hermes-Yi-34B [3]	75.79	72.43	78.14	58.87	60.42	67.96	70.67	64.00	63.09	72.17
Qwen2-VL-7B [6]	QwenLM-7B [5]	73.95	69.44	74.21	52.02	56.25	69.90	73.33	61.00	55.36	69.04
Qwen2.5-VL-7B [7]	Qwen2.5-7B [7]	71.59	67.55	73.43	53.63	58.33	73.79	74.67	56.00	61.85	68.38

**Table 3: Average  $CGLA_{\min}$  and  $CGLA_{\text{acc}}$  of open-source MLLMs on attributes derived from MM-SPUBENCH. Higher values in green indicate well-aligned attribute-anchor relations. Lower values in red indicate misalignment.**

MLLM	$CGLA_{\min}$		$CGLA_{\text{acc}}$ (%)	
	User	Asst.	User	Asst.
InternVL3-8B [90]	1.01	2.95	61.62	78.21
InternVL3-14B [90]	0.52	1.65	61.50	69.54
InternVL3-38B [90]	1.64	3.27	66.62	79.79
Llama-3.2-VI-11B [46]	1.67	2.40	63.75	71.29
LLaVA-v1.5-7B [39]	0.06	-0.06	60.38	38.46
LLaVA-v1.5-13B [39]	0.21	1.14	57.83	68.62
LLaVA-v1.6-mis-7B [39]	1.41	2.84	71.12	80.96
LLaVA-v1.6-vic-13B [39]	0.13	0.08	53.04	44.17
LLaVA-v1.6-34B [39]	0.16	1.68	52.92	71.29

the model output follows the choice format. Among open-source models, Llama3.2 [46] and LLaVA-v1.6 [39] models frequently fail to follow the instructions and produce text descriptions of their answers. To compensate for this, we concatenate the generation with “Choice:” and generate the next token only among the choice letters as their final answer. Detailed VQA prompts are included in the Appendix.

*Generative Likelihood Experiment.* From each VQA triplet of image, question, and choices, we obtain 3 spurious attributes and 1 core attribute, and perform generative evaluations on the quartet of image, object class, core attribute, and set of spurious attributes.

We formulate two chat templates, the User template and the Assistant template. The User template constructs a natural single-round open-ended visual chat task, where the user deliberately includes one attribute in the text input and asks about the type of the anchor object. The Assistant template follows a similar single-round open-ended visual chat task, where the user asks for observation in the image and the classification of the anchor object. In this template, the prefix of assistant generation is fixed to texts that establish a relationship between one attribute and the classification. The detailed templates are included in the Appendix. We use these two templates as the prompting function in Equation 3 and calculate the CGL of the given object label text under each attribute. The  $CGLA_{\min}$  is calculated following Equation 5 and  $CGLA_{\text{acc}}$  is calculated following Equation 6. The reported statistics are averaged over the dataset.

### 5.3 Main Results

*Overall VQA Accuracy on MM-SPUBENCH.* Based on the results in Table 2, we observe that MLLMs exhibit varying degrees of spurious bias. The most recent open-sourced model, InternVL3 [90], performs comparably to the best closed-sourced model tested. Across different types of spurious bias, we found significant variations in the MLLMs’ ability to address each type. They perform better in the BG and CO types, while their performance is notably subpar in the RS and Co1. types. This gap indicates that when prompted to choose the exact attribute that distinguishes a class of objects, MLLMs tend to fail more frequently when certain types of spurious attributes are present. Assuming the attribute selection of the MLLMs aligns with its implicit emergent reasoning process, we argue that certain attribute types are more tempting for the MLLMs, indicating the potential presence of such spurious biases in the MLLMs.

**Generative Likelihood Analysis.** The average conditional generation statistics are reported in Table 3, column text “User” and “Asst.” indicates the metric is computed with the *User prompt* template and the *Assistant prompt* template, respectively. We remove Qwen [6, 7] models from our experiments because they do not produce logits within the floating point range, making calculation impossible. In most models, the *Assistant prompt* template produced better alignment between the attributes and the anchor concept. We attribute this advantage to the more detailed and deliberate causal relationship in the *Assistant prompt*. Such a relationship is not applicable in the *User prompt* as the assistant’s prefix does not contain the attribute text. We notice that LLaVA-v1.5-7B [82] and LLaVA-v1.6-vic-13B [82] do not benefit from this stronger conditioning, which can be caused by possible failure in instruction-following or disturbance caused by the long custom assistant prefix. The *User prompt* provides a more natural evaluation, as the user can input arbitrary text in user-MLLM interactions. Based on the *User prompt* results, most models demonstrated, on average, a positive core condition advantage, with InternVL3-38B [90], Llama-3.2-VI-11B [46], and LLaVA-v1.6-mis-7B [82] performing the best. On per-instance confidence, these models show high  $CGLA_{\min}$  values greater than  $\log(4) \approx 1.38$ , indicating that on average these MLLMs generate the anchor text 4 times more likely when presented with a core attribute than with a spurious attribute. Focusing on preference alignment, these models demonstrated the highest  $CGLA_{\text{acc}}$  among tested models.

**Combined Analysis.** The overall performances of the MLLMs under the VQA test and the generative test are overall aligned, with the exceptions of LLaVA-v1.6-mis-7B [82] and InternVL-14B [90]. We see LLaVA-v1.6-mis-7B [82] performs well on generative test but produced low VQA accuracy. A slight difference between VQA and Generative tests may cause this discrepancy: the VQA test does not show the object anchor, whereas in the generative test, though the model is not exposed to the anchor when processing the attribute, the anchor information is given in the test pipeline. Therefore, the Generative test is an easier task, since the MLLMs do not need to resolve the true object class. Our argument is supported by higher accuracies across several models in Table 3. However, InternVL3-14B [90] is an exception. Its degraded accuracy from VQA to Generative test may indicate a misalignment of attributes and anchors that is not uncovered by high-level VQA testing, stressing the importance of generative evaluations.

#### 5.4 Visualization of Spurious Bias

To illustrate the influence of spurious features on MLLM reasoning and validate MM-SPUBENCH’s ability to reveal spurious biases learned by the models, we visualize Grad-CAM heatmaps [59] and token-level text attention heatmaps of LLaVA-v1.5-7B [82] and LLaVA-v1.5-13B [82] on examples in MM-SPUBENCH. We show one case in Fig. 4 and more visualizations in the Appendix. This example demonstrates that spurious attributes mislead the model. The Grad-CAM heatmaps pay more attention to irrelevant elements in the bathroom scene, such as the “toothpaste” and other background objects. Although the core feature of the object (the gripping structure) is present in the image, the model’s focus is dispersed across spurious features. The token-level text attention heatmap further



**Q:** Which feature best indicates the identity of the object near the toothpaste on the bathroom counter?

- A. The moist wipes
- B. The deodorant
- C. The object's gripping structure** ✓
- D. The toothpaste

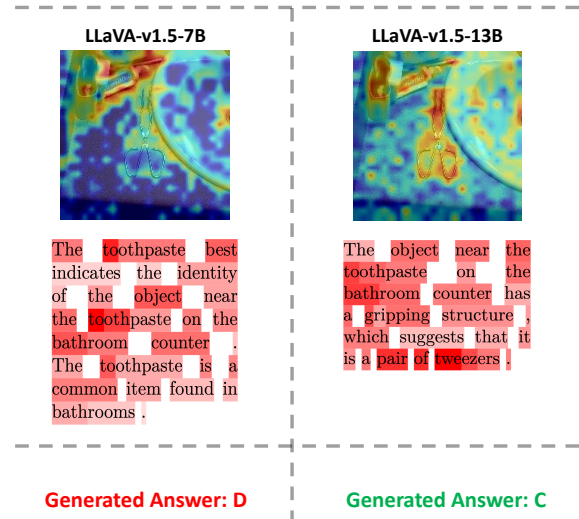


**Figure 4: GradCAM Visualization and Text Attention Heatmap of MM-SPUBENCH on LLaVA 7B and 13B. The anchor objects in the image is: tweezers.**

supports this observation, where generated text reasoning heavily emphasizes “bathroom” and other contextual elements. This agreement between visual and textual attention confirms that the model contains some spurious biases, which hinder it from learning the core attributes of the object and lead to incorrect predictions. Additionally, we show that increasing the model size from 7B to 13B can reduce the influence of spurious features to some extent. The 13B model reduces the focus on spurious attributes and focuses more on the core attribute “pair of tweezers”. However, we can still observe the focus of spurious attributes. It indicates that scaling alone is not sufficient to mitigate the impact of spurious correlations. This underscores the importance of our benchmark in evaluating and improving model robustness in complex multimodal scenarios.

#### 6 On Mitigating Spurious Correlation Effects

With MM-SPUBENCH, we explore the simple strategy of textual prompting as a preliminary investigation into the MLLMs’ implicit and explicit reasoning abilities as a key to mitigate spurious biases in multimodal question answering.

Following Lu et al. [41] and Li et al. [37], we explore simple prompting and evaluate its effectiveness in improving the performance of MLLMs on MM-SPUBENCH. We design and test three prompting strategies, namely: guiding, explain, and no-bias. The *guiding prompt* aims to break down the reasoning process and ask the MLLM to follow it. The *explain prompt* directly asks the

model to give reasons first and then provide an answer. The *no-bias prompt* reminds the MLLM not to fall for unrelated and spurious cues when answering. We show the prompt details in the Appendix Table 6. The idea is to implicitly or explicitly exploit the MLLMs' reasoning capacity to identify attributes that do not constitute the anchor's core features. The benchmark results for all tested model-prompt pairs are reported in Table 4, and per-category accuracy is reported in the Appendix. We exclude LLaVA-v1.6-34B [82] due to its prohibitive computational requirements for explicit reasoning.

The *vanilla prompt* yielded the best result for Qwen2-VL-7B [7]. For this model, longer self-generated contexts introduced by our prompt could distract them from the core information. In addition, lower *no-bias prompt* accuracy indicates limited implicit reasoning capacity. The *no-bias prompt* was effective for InternVL-3-8B [90], InternVL-3-14B [90], and LLaVA-1.6-vic-13B [82]. It works well for models with strong implicit reasoning ability that understand and follow meta-instructions about the decision-making process. The *explain prompt* is shown to increase the VQA accuracy of Llama-3.2-VI-11B [46]. It works best for models with strong explicit reasoning ability and long-context capacity. The *guiding prompt* improved the accuracy of InternVL-8B [90] the most, and it also improved the performance of Llama-3.2-VI-11B [46]. The rest of the tested models do not show significant performance gain from simple prompting, motivating research in advanced mitigation methods.

**Table 4: Overall Accuracy (%) by Model and Prompt Type.**

Model	Vanilla	Guiding	No Bias	Explain
InternVL3-8B [90]	71.92	<b>75.46</b>	74.96	72.67
InternVL3-14B [90]	77.92	74.88	<b>79.75</b>	76.96
InternVL3-38B [90]	83.04	82.62	<b>83.29</b>	82.96
Llama-3.2-VI-11B [46]	71.71	72.92	72.75	<b>74.25</b>
LLaVA-v1.5-7B [39]	39.54	39.62	38.38	<b>39.67</b>
LLaVA-v1.5-13B [39]	59.08	55.71	59.25	<b>59.75</b>
LLaVA-v1.6-mis-7B [39]	38.88	39.00	<b>39.08</b>	33.83
LLaVA-v1.6-vic-13B [39]	24.58	25.83	<b>38.04</b>	35.21
Qwen2-VL-7B [6]	<b>69.04</b>	56.71	67.04	65.46
Qwen2.5-VL-7B [7]	68.38	60.42	<b>68.79</b>	61.54

## 7 Conclusion

In this work, we systematically investigated the prevalence and impact of spurious biases in MLLMs. We introduced MM-SpuBENCH, a comprehensive benchmark designed to evaluate the robustness of MLLMs to spurious biases. This benchmark systematically measures how well these models distinguish between core and spurious features with two metrics, providing a useful framework for understanding and quantifying spurious biases. Our findings show that current MLLMs, particularly smaller models or those relying on basic modality alignment techniques, often fail to integrate visual and language modalities in multimodal tasks effectively. The evaluation results and visualization indicate that both open-source and proprietary MLLMs still rely on spurious correlations to various degrees, highlighting the need for improved multimodal alignment techniques and more robust architectures. We hope that MM-SpuBENCH

will drive further research in this field, leading to the development of more robust and reliable multimodal LLMs.

## Acknowledgments

This work is supported in part by the US National Science Foundation under grants CCF-2217071, CNS-2213700, IIS-2106913. Any opinions, findings, and conclusions or recommendations expressed in this material are those of the author(s) and do not necessarily reflect the views of the National Science Foundation.

## References

- [1] Abubakar Abid, Mert Yuksekgonul, and James Zou. 2022. Meaningfully debugging model mistakes using conceptual counterfactual explanations. In *ICML*. PMLR, 66–88.
- [2] Josh Achiam, Steven Adler, Sandhini Agarwal, Lama Ahmad, Ilge Akkaya, Florencia Leoni Aleman, Diogo Almeida, Janko Altenschmidt, Sam Altman, Shyamal Anadkat, et al. 2023. Gpt-4 technical report. *arXiv preprint arXiv:2303.08774* (2023).
- [3] 01 AI, Alex Young, Bei Chen, Chao Li, Chengen Huang, Ge Zhang, Guanwei Zhang, Heng Li, Jiangcheng Zhu, Jianqun Chen, Jing Chang, Kaidong Yu, Peng Liu, Qiang Liu, Shawn Yue, Senbin Yang, Shiming Yang, Tao Yu, Wen Xie, Wenhao Huang, Xiaohui Hu, Xiaoyi Ren, Xinyao Niu, Pengcheng Nie, Yuchi Xu, Yudong Liu, Yue Wang, Yuxuan Cai, Zhenyu Gu, Zhiyuan Liu, and Zonghong Dai. 2024. Yi: Open Foundation Models by 01.AI. *arXiv* (March 2024). doi:10.48550/arXiv.2403.04652
- [4] Anthropic. 2024. Claude 3 Family. <https://www.anthropic.com/news/claude-3-family>. Accessed: 2024-05-27.
- [5] Jinze Bai, Shuai Bai, Yunfei Chu, Zeyu Cui, Kai Dang, Xiaodong Deng, Yang Fan, Wenbin Ge, Yu Han, Fei Huang, Binyuan Hui, Luo Ji, Mei Li, Junyang Lin, Runji Lin, Dayiheng Liu, Gao Liu, Chengqiang Lu, Keming Lu, Jianxin Ma, Rui Men, Xingzhang Ren, Xuancheng Ren, Chuanqi Tan, Sinan Tan, Jianhong Tu, Peng Wang, Shijie Wang, Wei Wang, Shengguang Wu, Benfeng Xu, Jin Xu, An Yang, Hao Yang, Jian Yang, Shusheng Yang, Yang Yao, Bowen Yu, Hongyi Yuan, Zheng Yuan, Jianwei Zhang, Xingxuan Zhang, Yichang Zhang, Zhenru Zhang, Chang Zhou, Jingren Zhou, Xiaohuan Zhou, and Tianhang Zhu. 2023. Qwen Technical Report. *arXiv* (Sept. 2023). doi:10.48550/arXiv.2309.16609
- [6] Jinze Bai, Shuai Bai, Shusheng Yang, Shijie Wang, Sinan Tan, Peng Wang, Junyang Lin, Chang Zhou, and Jingren Zhou. 2023. Qwen-vl: A frontier large vision-language model with versatile abilities. *arXiv preprint arXiv:2308.12966* (2023).
- [7] Shuai Bai, Keqin Chen, Xuejing Liu, Jialin Wang, Wenbin Ge, Sibao Song, Kai Dang, Peng Wang, Shijie Wang, Jun Tang, Humen Zhang, Yuanzhi Zhu, Mingkun Yang, Zhaohai Li, Jianqiang Wan, Pengfei Wang, Wei Ding, Zheren Fu, Yiheng Xu, Jiabo Ye, Xi Zhang, Tianbao Xie, Zesen Cheng, Hang Zhang, Zhibo Yang, Haiyang Xu, and Junyang Lin. 2025. Qwen2.5-VL Technical Report. *arXiv preprint arXiv:2502.13923* (2025).
- [8] Zechen Bai, Pichao Wang, Tianjun Xiao, Tong He, Zongbo Han, Zheng Zhang, and Mike Zheng Shou. 2024. Hallucination of multimodal large language models: A survey. *arXiv preprint arXiv:2404.18930* (2024).
- [9] Oriol Barbany, Michael Huang, Xinliang Zhu, and Arnab Dhua. 2024. Leveraging Large Language Models for Multimodal Search. In *Proceedings of the IEEE/CVF Conference on Computer Vision and Pattern Recognition*. 1201–1210.
- [10] Andrei Barbu, David Mayo, Julian Alverio, William Luo, Christopher Wang, Dan Gutfreund, Josh Tenenbaum, and Boris Katz. 2019. ObjectNet: A large-scale bias-controlled dataset for pushing the limits of object recognition models. In *Advances in Neural Information Processing Systems*.
- [11] Anjanava Biswas and Wrick Talukdar. 2024. Robustness of Structured Data Extraction from In-Plane Rotated Documents Using Multi-Modal Large Language Models (LLM). *Journal of Artificial Intelligence Research* (2024).
- [12] Yonatan Bitton, Hritik Bansal, Jack Hessel, Rulin Shao, Wanrong Zhu, Anas Awadalla, Josh Gardner, Rohan Taori, and Ludwig Schimdt. 2023. Visit-bench: A benchmark for vision-language instruction following inspired by real-world use. *arXiv preprint arXiv:2308.06595* (2023).
- [13] Dongping Chen, Ruoxi Chen, Shilin Zhang, Yinyu Liu, Yaochen Wang, Huichi Zhou, Qihui Zhang, Pan Zhou, Yao Wan, and Lichao Sun. 2024. MLLM-as-a-Judge: Assessing Multimodal LLM-as-a-Judge with Vision-Language Benchmark. *arXiv preprint arXiv:2402.04788* (2024).
- [14] Aakanksha Chowdhery, Sharan Narang, Jacob Devlin, Maarten Bosma, Gaurav Mishra, Adam Roberts, Paul Barham, Hyung Won Chung, Charles Sutton, Sebastian Gehrmann, et al. 2023. Palm: Scaling language modeling with pathways. *Journal of Machine Learning Research* 24, 240 (2023), 1–113.
- [15] Hyung Won Chung, Le Hou, Shayne Longpre, Barret Zoph, Yi Tay, William Fedus, Yunxuan Li, Xuezhi Wang, Mostafa Dehghani, Siddhartha Brahma, et al. 2024.

- Scaling instruction-finetuned language models. *Journal of Machine Learning Research* 25, 70 (2024), 1–53.
- [16] Christopher Clark, Mark Yatskar, and Luke Zettlemoyer. 2019. Don't Take the Easy Way Out: Ensemble Based Methods for Avoiding Known Dataset Biases. In *Proceedings of the 2019 Conference on Empirical Methods in Natural Language Processing and the 9th International Joint Conference on Natural Language Processing (EMNLP-IJCNLP)*. 4069–4082.
- [17] Xuanming Cui, Alejandro Aparcedo, Young Kyun Jang, and Ser-Nam Lim. 2024. On the robustness of large multimodal models against image adversarial attacks. In *Proceedings of the IEEE/CVF Conference on Computer Vision and Pattern Recognition*. 24625–24634.
- [18] Wenliang Dai, Junnan Li, Dongxu Li, Anthony Meng Huat Tiong, Junqi Zhao, Weisheng Wang, Boyang Li, Pascale N Fung, and Steven Hoi. 2024. Instructblip: Towards general-purpose vision-language models with instruction tuning. *Advances in Neural Information Processing Systems* 36 (2024).
- [19] Jacob Devlin, Ming-Wei Chang, Kenton Lee, and Kristina Toutanova. 2018. Bert: Pre-training of deep bidirectional transformers for language understanding. *arXiv preprint arXiv:1810.04805* (2018).
- [20] Jacob Eisenstein. 2022. Informativeness and invariance: Two perspectives on spurious correlations in natural language. *arXiv preprint arXiv:2204.04487* (2022).
- [21] Paul Gavrikov, Jovita Lukaszik, Steffen Jung, Robert Geirhos, Bianca Lamm, Muhammad Jehanzeb Mirza, Margret Keuper, and Janis Keuper. 2024. Are Vision Language Models Texture or Shape Biased and Can We Steer Them? *arXiv preprint arXiv:2403.09193* (2024).
- [22] Robert Geirhos, Jörn-Henrik Jacobsen, Claudio Michaelis, Richard Zemel, Wieland Brendel, Matthias Bethge, and Felix A Wichmann. 2020. Shortcut learning in deep neural networks. *Nature Machine Intelligence* 2, 11 (2020), 665–673.
- [23] Robert Geirhos, Patricia Rubisch, Claudio Michaelis, Matthias Bethge, Felix A. Wichmann, and Wieland Brendel. 2019. ImageNet-trained CNNs are biased towards texture; increasing shape bias improves accuracy and robustness.. In *ICLR*. <https://openreview.net/forum?id=Bygh9j09KX>
- [24] Soumya Suvra Ghosal and Yixuan Li. 2024. Are Vision Transformers Robust to Spurious Correlations? *International Journal of Computer Vision* 132, 3 (2024), 689–709.
- [25] Tianyang Han, Qing Lian, Rui Pan, Renjie Pi, Jipeng Zhang, Shizhe Diao, Yong Lin, and Tong Zhang. 2024. The Instinctive Bias: Spurious Images lead to Hallucination in MLLMs. *arXiv preprint arXiv:2402.03757* (2024).
- [26] Kaiming He, Xinlei Chen, Saining Xie, Yanghao Li, Piotr Dollár, and Ross Girshick. 2022. Masked autoencoders are scalable vision learners. In *Proceedings of the IEEE/CVF conference on computer vision and pattern recognition*. 16000–16009.
- [27] Dan Hendrycks, Steven Basart, Norman Mu, Saurav Kadavath, Frank Wang, Evan Dorundo, Rahul Desai, Tyler Zhu, Samyak Parajuli, Mike Guo, et al. 2021. The many faces of robustness: A critical analysis of out-of-distribution generalization. In *Proceedings of the IEEE/CVF international conference on computer vision*. 8340–8349.
- [28] Dan Hendrycks and Thomas Dietterich. 2019. Benchmarking neural network robustness to common corruptions and perturbations. *arXiv preprint arXiv:1903.12261* (2019).
- [29] Dan Hendrycks, Kevin Zhao, Steven Basart, Jacob Steinhardt, and Dawn Song. 2021. Natural adversarial examples. In *CVPR*. 15262–15271.
- [30] Parsa Hosseini, Sumit Nawathe, Mazda Moayeri, Sriram Balasubramanian, and Soheil Feizi. 2025. Seeing What's Not There: Spurious Correlation in Multimodal LLMs. *arXiv preprint arXiv:2503.08884* (2025).
- [31] Qidong Huang, Xiaoyi Dong, Pan Zhang, Bin Wang, Conghui He, Jiaqi Wang, Dahua Lin, Weiming Zhang, and Nenghai Yu. 2023. Opera: Alleviating hallucination in multi-modal large language models via over-trust penalty and retrospection-allocation. *arXiv preprint arXiv:2311.17911* (2023).
- [32] Shaohan Huang, Li Dong, Wenhui Wang, Yaru Hao, Saksham Singhal, Shuming Ma, Tengchao Lv, Lei Cui, Owais Khan Mohammed, Barun Patra, et al. 2023. Language is not all you need: Aligning perception with language models. *Advances in Neural Information Processing Systems* 36 (2023), 72096–72109.
- [33] Drew A Hudson and Christopher D Manning. 2019. Gqa: A new dataset for real-world visual reasoning and compositional question answering. In *Proceedings of the IEEE/CVF conference on computer vision and pattern recognition*. 6700–6709.
- [34] Albert Q. Jiang, Alexandre Sablayrolles, Arthur Mensch, Chris Bamford, Devendra Singh Chaplot, Diego de las Casas, Florian Bressand, Gianna Lengyel, Guillaume Lample, Lucile Saulnier, Léo Renard Lavaud, Marie-Anne Lachaux, Pierre Stock, Teven Le Scao, Thibaut Lavril, Thomas Wang, Timothée Lacroix, and William El Sayed. 2023. Mistral 7B. *arXiv* (Oct. 2023). doi:10.48550/arXiv.2310.06825
- [35] Polina Kirichenko, Pavel Izmailov, and Andrew Gordon Wilson. 2023. Last Layer Re-Training is Sufficient for Robustness to Spurious Correlations. In *ICLR*. <https://openreview.net/forum?id=Zb6c8A-Fghk>
- [36] Yifan Li, Yifan Du, Kun Zhou, Jinpeng Wang, Wayne Xin Zhao, and Ji-Rong Wen. 2023. Evaluating object hallucination in large vision-language models. *arXiv preprint arXiv:2305.10355* (2023).
- [37] Yijiang Li, Qingying Gao, Tianwei Zhao, Bingyang Wang, Haoran Sun, Haiyun Lyu, Dezhi Luo, and Hokin Deng. 2025. Core Knowledge Deficits in Multi-Modal Language Models. *arXiv preprint arXiv:2410.10855* (2025).
- [38] Evan Z Liu, Behzad Haghgoo, Annie S Chen, Aditi Raghunathan, Pang Wei Koh, Shiori Sagawa, Percy Liang, and Chelsea Finn. 2021. Just train twice: Improving group robustness without training group information. In *ICML*. PMLR, 6781–6792.
- [39] Haotian Liu, Chunyuan Li, Qingyang Wu, and Yong Jae Lee. 2024. Visual instruction tuning. *Advances in neural information processing systems* 36 (2024).
- [40] Yuan Liu, Haodong Duan, Yuanhan Zhang, Bo Li, Songyang Zhang, Wangbo Zhao, Yike Yuan, Jiaqi Wang, Conghui He, Ziwei Liu, et al. 2023. Mmbench: Is your multi-modal model an all-around player? *arXiv preprint arXiv:2307.06281* (2023).
- [41] Zeyu Lu, Di Huang, Lei Bai, Jingjing Qu, Chengyue Wu, Xihui Liu, and Wanli Ouyang. 2024. Seeing is not always believing: Benchmarking human and model perception of ai-generated images. *Advances in Neural Information Processing Systems* 36 (2024).
- [42] Jinqi Luo, Zhaoning Wang, Chen Henry Wu, Dong Huang, and Fernando De la Torre. 2023. Zero-shot model diagnosis. In *Proceedings of the IEEE/CVF Conference on Computer Vision and Pattern Recognition*. 11631–11640.
- [43] Brandon McKinzie, Zhe Gan, Jean-Philippe Fauconnier, Sam Dodge, Bowen Zhang, Philipp Dufter, Dhruvi Shah, Xianzhi Du, Futang Peng, Floris Weers, et al. 2024. Mm1: Methods, analysis & insights from multimodal llm pre-training. *arXiv preprint arXiv:2403.09611* (2024).
- [44] Emily McMilin. 2022. Selection Bias Induced Spurious Correlations in Large Language Models. In *ICML 2022: Workshop on Spurious Correlations, Invariance and Stability*. <https://openreview.net/forum?id=8nnaDv9dUli>
- [45] AI Meta. 2024. Introducing Llama 3.1: Our most capable models to date. <https://ai.meta.com/blog/meta-llama-3-1/>
- [46] AI Meta. 2024. Llama 3.2: Revolutionizing edge AI and vision with open, customizable models. <https://ai.meta.com/blog/llama-3-2-connect-2024-vision-edge-mobile-devices/>
- [47] Yifei Ming, Hang Yin, and Yixuan Li. 2022. On the impact of spurious correlation for out-of-distribution detection. In *Proceedings of the AAAI conference on artificial intelligence*, Vol. 36. 10051–10059.
- [48] Junhyun Nam, Jaehyung Kim, Jaeho Lee, and Jinwoo Shin. 2022. Spread Spurious Attribute: Improving Worst-group Accuracy with Spurious Attribute Estimation. In *ICLR*. [https://openreview.net/forum?id=\\_F9xpOrqyX9](https://openreview.net/forum?id=_F9xpOrqyX9)
- [49] Meike Nauta, Ricky Walsh, Adam Dubowski, and Christin Seifert. 2021. Uncovering and correcting shortcut learning in machine learning models for skin cancer diagnosis. *Diagnostics* 12, 1 (2021), 40.
- [50] Besmira Nushi, Ece Kamar, and Eric Horvitz. 2018. Towards accountable ai: Hybrid human-machine analyses for characterizing system failure. In *Proceedings of the AAAI Conference on Human Computation and Crowdsourcing*, Vol. 6. 126–135.
- [51] Maxime Oquab, Timothée Darcet, Théo Moutakanni, Huy Vo, Marc Szafraniec, Vasil Khalidov, Pierre Fernandez, Daniel Haziza, Francisco Massa, Alaaeldin El-Nouby, et al. 2023. Dinov2: Learning robust visual features without supervision. *arXiv preprint arXiv:2304.07193* (2023).
- [52] Gregory Plumb, Marco Tulio Ribeiro, and Ameet Talwalkar. 2022. Finding and Fixing Spurious Patterns with Explanations. *Transactions on Machine Learning Research* (2022). <https://openreview.net/forum?id=whJpUgmP5l> Expert Certification.
- [53] Viraj Prabhu, Sriram Yenamandra, Prithvijit Chattopadhyay, and Judy Hoffman. 2023. Lance: Stress-testing visual models by generating language-guided counterfactual images. *Advances in Neural Information Processing Systems* 36 (2023), 25165–25184.
- [54] Haonan Qiu, Chaowei Xiao, Lei Yang, Xinchun Yan, Honglak Lee, and Bo Li. 2020. Semanticadv: Generating adversarial examples via attribute-conditioned image editing. In *Computer Vision—ECCV 2020: 16th European Conference, Glasgow, UK, August 23–28, 2020, Proceedings, Part XIV 16*. Springer, 19–37.
- [55] Alec Radford, Jong Wook Kim, Chris Hallacy, Aditya Ramesh, Gabriel Goh, Sandhini Agarwal, Girish Sastry, Amanda Askell, Pamela Mishkin, Jack Clark, et al. 2021. Learning transferable visual models from natural language supervision. In *International conference on machine learning*. PMLR, 8748–8763.
- [56] Hanoona Rasheed, Muhammad Maaz, Sahal Shaji, Abdelrahman Shaker, Salman Khan, Hisham Cholakkal, Rao M Anwer, Eric Xing, Ming-Hsuan Yang, and Fahad S Khan. 2024. Glamm: Pixel grounding large multimodal model. In *Proceedings of the IEEE/CVF Conference on Computer Vision and Pattern Recognition*. 13009–13018.
- [57] Shiori Sagawa, Pang Wei Koh, Tatsunori B Hashimoto, and Percy Liang. 2019. Distributionally Robust Neural Networks. In *ICLR*.
- [58] Shiori Sagawa, Aditi Raghunathan, Pang Wei Koh, and Percy Liang. 2020. An investigation of why overparameterization exacerbates spurious correlations. In *ICML*. PMLR, 8346–8356.
- [59] Ramprasaath R Selvaraju, Michael Cogswell, Abhishek Das, Ramakrishna Vedantam, Devi Parikh, and Dhruv Batra. 2020. Grad-CAM: visual explanations from deep networks via gradient-based localization. *International Journal of Computer Vision* 128 (2020), 336–359.

- [60] Amanpreet Singh, Vivek Natarajan, Meet Shah, Yu Jiang, Xinlei Chen, Dhruv Batra, Devi Parikh, and Marcus Rohrbach. 2019. Towards vqa models that can read. In *Proceedings of the IEEE/CVF conference on computer vision and pattern recognition*. 8317–8326.
- [61] Mohammad Reza Taesiri, Giang Nguyen, Sarra Habchi, Cor-Paul Bezemer, and Anh Nguyen. 2023. Zoom is what you need: An empirical study of the power of zoom and spatial biases in image classification. *arXiv preprint arXiv:2304.05538* (2023).
- [62] Gemini Team, Rohan Anil, Sebastian Borgeaud, Yonghui Wu, Jean-Baptiste Alayrac, Jiahui Yu, Radu Soricut, Johan Schalkwyk, Andrew M Dai, Anja Hauth, et al. 2023. Gemini: a family of highly capable multimodal models. *arXiv preprint arXiv:2312.11805* (2023).
- [63] Shengbang Tong, Zhuang Liu, Yuexiang Zhai, Yi Ma, Yann LeCun, and Saining Xie. 2024. Eyes wide shut? exploring the visual shortcomings of multimodal llms. *arXiv preprint arXiv:2401.06209* (2024).
- [64] Hugo Touvron, Thibaut Lavril, Gautier Izacard, Xavier Martinet, Marie-Anne Lachaux, Timothée Lacroix, Baptiste Rozière, Naman Goyal, Eric Hambro, Faisal Azhar, et al. 2023. Llama: Open and efficient foundation language models. *arXiv preprint arXiv:2302.13971* (2023).
- [65] Hugo Touvron, Louis Martin, Kevin Stone, Peter Albert, Amjad Almahairi, Yasmine Babaei, Nikolay Bashlykov, Soumya Batra, Prajwal Bhargava, Shruti Bhosale, Dan Bikel, Lukas Blecher, Cristian Canton Ferrer, Moya Chen, Guillem Cucurull, David Esch, Jude Fernandes, Jeremy Fu, Wenyin Fu, Brian Fuller, Cynthia Gao, Vedanuj Goswami, Naman Goyal, Anthony Hartshorn, Saghar Hosseini, Rui Hou, Hakan Inan, Marcin Kardas, Viktor Kerkez, Madian Khabsa, Isabel Kloumann, Artem Korenev, Punit Singh Koura, Marie-Anne Lachaux, Thibaut Lavril, Jenya Lee, Diana Liskovich, Yinghai Lu, Yuning Mao, Xavier Martinet, Todor Mihaylov, Pushkar Mishra, Igor Molybog, Yixin Nie, Andrew Poulton, Jeremy Reizenstein, Rashi Rungta, Kalyan Saladi, Alan Schelten, Ruan Silva, Eric Michael Smith, Ranjan Subramanian, Xiaoqing Ellen Tan, Binh Tang, Ross Taylor, Adina Williams, Jian Xiang Kuan, Puxin Xu, Zheng Yan, Iliyan Zarov, Yuchen Zhang, Angela Fan, Melanie Kambadur, Sharan Narang, Aurelien Rodriguez, Robert Stojnic, Sergey Edunov, and Thomas Scialom. 2023. Llama 2: Open Foundation and Fine-Tuned Chat Models. *arXiv* (2023). doi:10.48550/arXiv.2307.09288
- [66] Haohan Wang, Songwei Ge, Zachary Lipton, and Eric P Xing. 2019. Learning robust global representations by penalizing local predictive power. *Advances in Neural Information Processing Systems* 32 (2019).
- [67] Tianlu Wang, Rohit Sridhar, Diyi Yang, and Xuezhi Wang. 2022. Identifying and Mitigating Spurious Correlations for Improving Robustness in NLP Models. In *Findings of the Association for Computational Linguistics: NAACL 2022*. 1719–1729.
- [68] Zefeng Wang, Zhen Han, Shuo Chen, Fan Xue, Zifeng Ding, Xun Xiao, Volker Tresp, Philip Torr, and Jindong Gu. 2024. Stop Reasoning! When Multimodal LLMs with Chain-of-Thought Reasoning Meets Adversarial Images. *arXiv preprint arXiv:2402.14899* (2024).
- [69] Jason Wei, Maarten Bosma, Vincent Y Zhao, Kelvin Guu, Adams Wei Yu, Brian Lester, Nan Du, Andrew M Dai, and Quoc V Le. 2021. Finetuned language models are zero-shot learners. *arXiv preprint arXiv:2109.01652* (2021).
- [70] Penghao Wu and Saining Xie. 2023. V\*: Guided Visual Search as a Core Mechanism in Multimodal LLMs. *arXiv preprint arXiv:2312.14135* (2023).
- [71] Shirley Wu, Mert Yuksekogonul, Linjun Zhang, and James Zou. 2023. Discover and Cure: Concept-aware Mitigation of Spurious Correlation. *arXiv preprint arXiv:2305.00650* (2023).
- [72] Kai Xiao, Logan Engstrom, Andrew Ilyas, and Aleksander Madry. 2021. Noise or Signal: The Role of Image Backgrounds in Object Recognition. In *ICLR*.
- [73] Yihao Xue, Siddharth Joshi, Dang Nguyen, and Baharan Mirzasoleiman. 2024. Understanding the Robustness of Multi-modal Contrastive Learning to Distribution Shift. In *The Twelfth International Conference on Learning Representations*.
- [74] Yu Yang, Besmira Nushi, Hamid Palangi, and Baharan Mirzasoleiman. 2023. Mitigating spurious correlations in multi-modal models during fine-tuning. In *International Conference on Machine Learning*. PMLR, 39365–39379.
- [75] Yuzhe Yang, Haoran Zhang, Dina Katabi, and Marzyeh Ghassemi. 2023. Change is hard: a closer look at subpopulation shift. In *Proceedings of the 40th International Conference on Machine Learning*. 39584–39622.
- [76] Wenqian Ye, Di Wang, Guangtao Zheng, Bohan Liu, and Aidong Zhang. 2026. SAGE: Spuriousness-Aware Guided Prompt Exploration for Mitigating Multimodal Bias. *AAAI Conference on Artificial Intelligence (AAAI)* (2026).
- [77] Wenqian Ye, Guangtao Zheng, Xu Cao, Yunsheng Ma, and Aidong Zhang. 2024. Spurious Correlations in Machine Learning: A Survey. *arXiv preprint arXiv:2402.12715* (2024).
- [78] Zhenfei Yin, Jiong Wang, Jianjian Cao, Zhelun Shi, Dingning Liu, Mukai Li, Xiaoshui Huang, Zhiyong Wang, Lu Sheng, Lei Bai, et al. 2024. Lamm: Language-assisted multi-modal instruction-tuning dataset, framework, and benchmark. *Advances in Neural Information Processing Systems* 36 (2024).
- [79] Lin Yong, Lu Tan, Hao Yifan, Ho Nam Wong, Hanze Dong, Weizhong Zhang, Yujin Yang, and Tong Zhang. 2023. Spurious Feature Diversification Improves Out-of-distribution Generalization. In *The Twelfth International Conference on Learning Representations*.
- [80] Weihao Yu, Zhengyuan Yang, Linjie Li, Jianfeng Wang, Kevin Lin, Zicheng Liu, Xinchao Wang, and Lijuan Wang. 2023. Mm-vet: Evaluating large multimodal models for integrated capabilities. *arXiv preprint arXiv:2308.02490* (2023).
- [81] Yuexiang Zhai, Shengbang Tong, Xiao Li, Mu Cai, Qing Qu, Yong Jae Lee, and Yi Ma. 2024. Investigating the Catastrophic Forgetting in Multimodal Large Language Model Fine-Tuning. In *Conference on Parsimony and Learning*. PMLR, 202–227.
- [82] Hao Zhang, Hongyang Li, Feng Li, Tianhe Ren, Xueyan Zou, Shilong Liu, Shijia Huang, Jianfeng Gao, Chunyuan Li, Jainwei Yang, et al. 2025. Llava-grounding: Grounded visual chat with large multimodal models. In *European Conference on Computer Vision*. Springer, 19–35.
- [83] Jiawei Zhang, Yang Wang, Piero Molino, Lezhi Li, and David S Ebert. 2018. Manifold: A model-agnostic framework for interpretation and diagnosis of machine learning models. *IEEE transactions on visualization and computer graphics* 25, 1 (2018), 364–373.
- [84] Susan Zhang, Stephen Roller, Naman Goyal, Mikel Artetxe, Moya Chen, Shuohui Chen, Christopher Dewan, Mona Diab, Xian Li, Xi Victoria Lin, et al. 2022. Opt: Open pre-trained transformer language models. *arXiv preprint arXiv:2205.01068* (2022).
- [85] Guangtao Zheng, Wenqian Ye, and Aidong Zhang. 2024. Benchmarking spurious bias in few-shot image classifiers. In *European Conference on Computer Vision*. Springer, 346–364.
- [86] Guangtao Zheng, Wenqian Ye, and Aidong Zhang. 2024. Learning Robust Classifiers with Self-Guided Spurious Correlation Mitigation. In *The 33rd International Joint Conference on Artificial Intelligence*.
- [87] Guangtao Zheng, Wenqian Ye, and Aidong Zhang. 2024. Spuriousness-aware meta-learning for learning robust classifiers. In *Proceedings of the 30th ACM SIGKDD Conference on Knowledge Discovery and Data Mining*. 4524–4535.
- [88] Lianmin Zheng, Wei-Lin Chiang, Ying Sheng, Siyuan Zhuang, Zhaohao Wu, Yonghao Zhuang, Zi Lin, Zhuohan Li, Dacheng Li, Eric P. Xing, Hao Zhang, Joseph E. Gonzalez, and Ion Stoica. 2023. Judging LLM-as-a-Judge with MT-Bench and Chatbot Arena. In *NeurIPS Datasets and Benchmarks Track*. doi:10.48550/arXiv.2306.05685
- [89] Didi Zhu, Zhongyi Sun, Zexi Li, Tao Shen, Ke Yan, Shouhong Ding, Kun Kuang, and Chao Wu. 2024. Model Tailor: Mitigating Catastrophic Forgetting in Multimodal Large Language Models. *arXiv preprint arXiv:2402.12048* (2024).
- [90] Jinguo Zhu, Weiyun Wang, Zhe Chen, Zhaoyang Liu, Shenglong Ye, Lixin Gu, Hao Tian, Yuchen Duan, Weijie Su, Jie Shao, Zhangwei Gao, Erfei Cui, Xuehui Wang, Yue Cao, Yangzhou Liu, Xingguang Wei, Hongjie Zhang, Haomin Wang, Weiye Xu, Hao Li, Jiahao Wang, Nianchen Deng, Songze Li, Yinan He, Tan Jiang, Jiapeng Luo, Yi Wang, Conghui He, Botian Shi, Xingcheng Zhang, Wenqi Shao, Junjun He, Yingdong Xiong, Wenwen Qu, Peng Sun, Penglong Jiao, Han Lv, Lijun Wu, Kaipeng Zhang, Huipeng Deng, Jiaye Ge, Kai Chen, Limin Wang, Min Dou, Lewei Lu, Xizhou Zhu, Tong Lu, Dahua Lin, Yu Qiao, Jifeng Dai, and Wenhui Wang. 2025. InternVL3: Exploring Advanced Training and Test-Time Recipes for Open-Source Multimodal Models. *arXiv:2504.10479*

## Appendix

### A More Information of the Data

#### A.1 Public Availability

The MM-SpuBENCH dataset is publicly accessible at <https://huggingface.co/datasets/mmbench/MM-SpuBench>. The benchmark is licensed under the MIT License; however, users should refer to the licenses of the individual data sources outlined in the following section. The benchmark will be continuously updated to incorporate new developments and feedback from the community. Benchmark construction and evaluation code are included in the supplementary material, and the repository will be made available on GitHub after the anonymous review period. For a more comprehensive understanding of the benchmark, additional data instances are provided in Table 8 and Table 9. Detailed descriptions and examples of the spurious correlation types defined in the main paper are available in Table 5.

#### A.2 Data Sources and Licenses

*ObjectNet*. ObjectNet is a vision dataset with 50,000 images, specifically designed to test object recognition systems under varied

**Table 5: Types of spurious correlations categorized in MM-SpUBENCH.**

Type	Description
Background (BG)	Occurs when the model relies on background context instead of the subject, e.g., identifying animals by natural backgrounds and failing in urban settings.
Texture and Noise (TN)	Arises when the model focuses on textures or noise patterns instead of shapes. E.g., misclassifying fruits due to changes in surface texture.
Co-occurring Objects (CO)	Happens when the model associates frequently appearing objects together. E.g., labeling any scene with a microwave as a kitchen.
Relative Size (RS)	Occurs when the model uses the relative size of objects as a cue. E.g., misclassifying a toy car as a real car due to a close-up perspective.
Colorization (Col.)	Related to reliance on specific colors for predictions. E.g., failing to recognize bananas that are green or brown.
Orientation (Ori.)	Arises when the model depends on the orientation of objects. E.g., struggling with faces not shown upright or from side profiles.
Lighting and Shadows (LS)	Occurs when predictions are influenced by lighting conditions or shadows. E.g., misclassifying objects in images with different lighting conditions.
Perspective and Angle (PA)	Emerges when the model relies on the viewing angle of objects. E.g., car recognition failing with top-down or oblique views.
Shape (Sha.)	Arises when an object has an unusual shape resembling another object. E.g., misidentifying a deformed fruit as a different type due to shape similarity.

conditions. It includes 313 object classes and controls for rotation, background, and viewpoint. This dataset reveals significant performance drops, showing real-world challenges and difficulties in transfer learning. ObjectNet is free for both research and commercial use, with the following restrictions:

- (1) ObjectNet cannot be used to tune the parameters of any model.
- (2) Individual images from ObjectNet must include their 1-pixel red border when posted online.

The license details can be found at <https://objectnet.dev/download.html>.

*ImageNet*. ImageNet is a comprehensive visual database used for visual object recognition research, containing millions of labeled images across thousands of categories. It serves as a key benchmark for evaluating computer vision algorithms and advancing deep learning research. The license details for ImageNet are available at <https://www.image-net.org/download.php>.

*ImageNet-R(edition)*. ImageNet-R is a subset of ImageNet-1K classes with art, cartoons, graffiti, embroidery, graphics, origami, paintings, patterns, plastic objects, plush objects, sculptures, sketches, tattoos, toys, and video game renditions of ImageNet classes. It contains renditions of 200 ImageNet classes, with a total of 30,000 images. This dataset is available under the MIT License at <https://github.com/hendrycks/imagenet-r>.

*ImageNet-A*. ImageNet-A contains real-world, unmodified examples that cause significant performance degradation in machine learning models. The dataset is available under the MIT License at <https://github.com/hendrycks/natural-adv-examples>.

*ImageNet-C*. The ImageNet-C dataset consists of 15 types of corruptions applied to ImageNet validation images, categorized into noise, blur, weather, and digital, each with five severity levels,

resulting in 75 distinct corruptions. This dataset is available under the Apache License 2.0 at <https://github.com/hendrycks/robustness>.

*ImageNet-Sketch*. ImageNet-Sketch includes 50,000 images, with 50 sketches for each of the 1,000 ImageNet classes. These images are gathered using Google Image searches with the query "sketch of CLASS" in black and white. The dataset is under the MIT License at <https://github.com/HaohanWang/ImageNet-Sketch>.

*ImageNet-Real*. ImageNet-Real offers "Re-Assessed" (Real) labels with multi-label and more accurate annotations from the "Are we done with ImageNet" paper. The dataset is available under the Apache License 2.0 at <https://github.com/google-research/reassessed-imagenet>.

*ImageNet-Hard*. ImageNet-Hard is a new benchmark featuring challenging images curated from various ImageNet validation datasets. It challenges state-of-the-art vision models as simply zooming in often fails to improve classification accuracy. The dataset is available under the MIT License at <https://github.com/taesiri/ZoomIsAllYouNeed>.

## B Disuccsion on Definition 3.1

Building on Section 3.2 and Definition 3.1, we explore how spurious biases learned in the vision encoder and the LLM can propagate into MLLMs. To analyze this, we represent the training data probabilities in the vision encoder and LLM of the MLLM using a spurious attribute  $z$ , the core object  $c$ , and the core features  $x_{core}$  and  $y_{core}$  as follows.

$$\text{In Vision Encoder: } p(z|c, x_{core}) \gg p(z|x_{core}) \quad (7)$$

$$\text{In LLM: } p(z|c, y_{core}) \gg p(z|y_{core}) \quad (8)$$

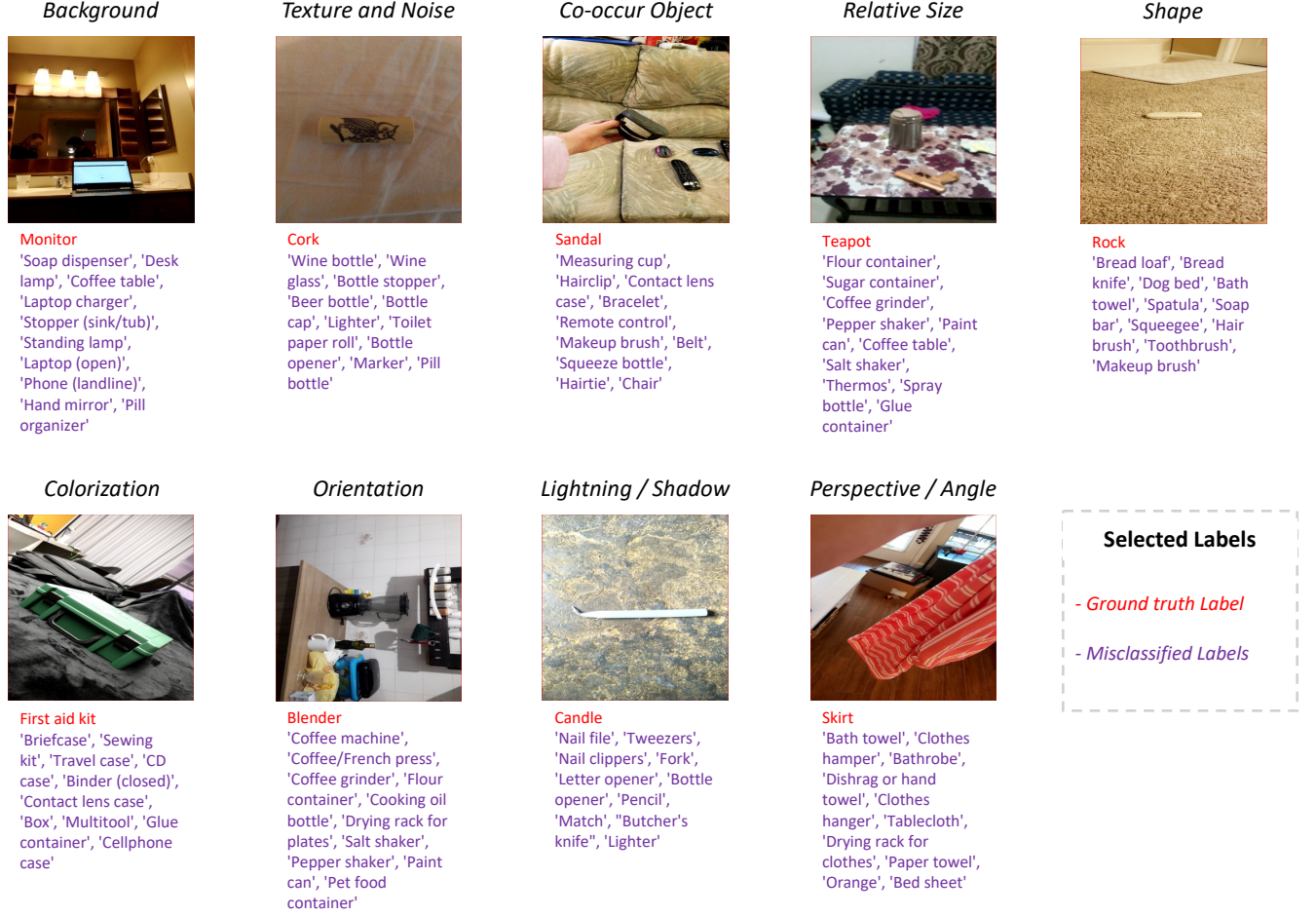


Figure 5: Examples of ground truth and misclassified labels after zero-shot classification. The red color shows the ground truth label and the purple color shows 10 misclassified labels selected by our method.

The conditional probability on the spurious attribute  $z$ , given the core features and object, is:

$$p(z|x_{\text{core}}, y_{\text{core}}, c) = \frac{p(x_{\text{core}}, y_{\text{core}}|z, c)p(z|c)}{p(x_{\text{core}}, y_{\text{core}}|c)} \quad (9)$$

$$= \frac{p(x_{\text{core}}|z, c)p(y_{\text{core}}|z, c)p(z|c)}{p(x_{\text{core}}|c)p(y_{\text{core}}|c)} \quad (10)$$

$$= \frac{p(z|x_{\text{core}}, c)p(z|y_{\text{core}}, c)p(z|c)}{p(z|c)p(z|c)} \quad (11)$$

$$= \frac{p(z|x_{\text{core}}, c)p(z|y_{\text{core}}, c)}{p(z)} \quad (12)$$

Without considering the core object  $c$ , the conditional probability on the spurious attribute  $z$  is:

$$p(z|x_{\text{core}}, y_{\text{core}}) = \frac{p(x_{\text{core}}, y_{\text{core}}|z)p(z)}{p(x_{\text{core}}, y_{\text{core}})} \quad (13)$$

$$= \frac{p(x_{\text{core}}|z)p(y_{\text{core}}|z)p(z)}{p(x_{\text{core}}, y_{\text{core}})} \quad (14)$$

$$= \frac{p(z|x_{\text{core}})p(z|y_{\text{core}})p(z)p(x_{\text{core}})p(y_{\text{core}})}{p(z)p(z)p(x_{\text{core}}, y_{\text{core}})} \quad (15)$$

$$= \frac{p(z|x_{\text{core}})p(z|y_{\text{core}})}{p(z)} \cdot \frac{p(x_{\text{core}})p(y_{\text{core}})}{p(x_{\text{core}}, y_{\text{core}})} \quad (16)$$

$$\approx \frac{p(z|x_{\text{core}})p(z|y_{\text{core}})}{p(z)} \quad (17)$$

By (7) and (8), we can get inequality (1) in the multimodal case.

$$p(\mathbf{z}|x_{\text{core}}, c)p(\mathbf{z}|y_{\text{core}}, c) \gg p(\mathbf{z}|x_{\text{core}})p(\mathbf{z}|y_{\text{core}}) \quad (18)$$

$$\frac{p(\mathbf{z}|x_{\text{core}}, c)p(\mathbf{z}|y_{\text{core}}, c)}{p(\mathbf{z})} \gg \frac{p(\mathbf{z}|x_{\text{core}})p(\mathbf{z}|y_{\text{core}})}{p(\mathbf{z})} \quad (19)$$

$$p(\mathbf{z}|x_{\text{core}}, y_{\text{core}}, c) \gg p(\mathbf{z}|x_{\text{core}}, y_{\text{core}}) \quad (20)$$

We show that multimodal spurious biases can be exacerbated in the vision and language modalities. In this work, we assume *the case that the spurious attribute  $\mathbf{z}$  is shared between the vision encoder and LLMs*. Future work could explore more complex scenarios where the spurious attribute is not shared and investigate whether such cases further impact the robustness of MLLMs.

## C More Experimental Details

### C.1 Zero-shot Classification

In this section, we demonstrate that, in our designed image pre-selection stage, zero-shot classification using CLIP can effectively identify images with spurious correlations. This phenomenon has been previously observed and supported in several works. For instance, Table 4 in [73] reports that the pretrained CLIP model, using the ViT-L/14@336px backbone, exhibited significantly lower worst-group accuracy (34.0%) compared to average accuracy (88.5%). However, the underperformance of CLIP models may also stem from factors such as label noise or annotation errors. To address this, we select images where CLIP’s true class prediction is not in the top- $k$  but appears in the top- $l$ , allowing us to focus on potential spurious correlations.

We chose the CLIP model for zero-shot classification for several reasons. CLIP is widely adopted as a vision encoder in many of the most popular open-source MLLMs, such as LLaVA, which we use as baseline methods in Table 2. Moreover, this paper highlights the potential for simple modality alignment methods to propagate spurious biases from the vision encoder to the broader MLLM framework. In Section 3.2, we provide evidence of how spurious biases observed in CLIP models can influence the entire MLLM pipeline, showing the relevance of addressing these biases at the source to enhance overall robustness.

As shown in Fig. 5, misclassified labels often include spurious information unrelated to the core object but present in the image or contextually linked to it (e.g., ‘Cork’ vs. ‘Wine Bottle’). This supports the effectiveness of zero-shot classification in identifying potential spurious attributes. Zero-shot classification enables models to predict without prior exposure to specific examples, and analyzing misclassified labels helps reveal spurious attributes tied to the ground truth label. For instance, ‘Cork’ is frequently misclassified as ‘Wine Bottle’ or ‘Wine Glass,’ highlighting the model’s reliance on contextual cues over intrinsic features. Using CLIP-ViT-L/14@336px<sup>1</sup>, we identified specific spurious correlations that degrade model performance. For example, ‘Monitor’ was confused with ‘Soap Dispenser’ or ‘Desk Lamp’ due to background features, while ‘Sandal’ was misclassified as ‘Measuring Cup’ or ‘Hairclip’ due to similarities in shape and orientation.

### C.2 Prompt Engineering

To ensure the effective generation and evaluation of questions for analyzing spurious correlations in images, we design the prompts for the MLLMs. In Fig. 7, we created a system message prompt to guide the assistant in identifying spurious correlations and deriving core and spurious attributes. We then formulate multiple-choice questions that test a model’s ability to distinguish these attributes. This ensures challenging and accurately reflective questions of spurious biases.

For zero-shot evaluation on open-source models, as shown in Fig. 8, we directly ask the model to select the best answer. In contrast, for closed-source models, as illustrated in Fig. 9, we designed a straightforward prompt instructing the assistant to answer questions based on the provided image and four answer options, focusing on selecting the best answer and providing a brief explanation. Some open-source models may not consistently follow instructions and provide answers in the correct format. To address this, we do not explicitly require these models to include reasoning in their responses. However, for proprietary models, we ask them to first provide a brief explanation of their reasoning in one sentence before generating the final answer. This approach ensures that the models better comprehend and address the visual question-answering (VQA) task.

Additionally, we used the chain-of-thought prompt to enhance the assistant’s reasoning capability by considering the type of spurious correlation provided in the benchmark and thinking step-by-step before choosing the best answer in Fig. 10. In this work, we only use a simple strategy with two steps to do chain-of-thought reasoning, as we don’t want to expose too much information to make the benchmark less challenging. However, in practice, it is recommended to use the concept information (core and spurious attributes) as mentioned in our benchmark to guide the MLLMs with better focus, as long as we determine the anchor object in the data. Our experiments serve as a motivating example for future research to develop improved strategies for enhancing the robustness of MLLMs to spurious biases.

### C.3 Visualization Details

In this section, we provide the experimental details of the visualizations and additional Grad-CAM visualizations and text attention heatmaps of MM-SPUBENCH on LLaVA 7B and 13B, as shown in Fig. 6. For these visualizations, we prompted the MLLMs to reason through their generated answers using the template provided in Fig. 12. We limited the generated outputs to a maximum of 50 tokens for clarity and excluded truncated sentences. For the Grad-CAM visualizations, we selected the last two layers of the LLaVA vision encoder to analyze the model’s visual focus and understand its interpretation of the input. For the text attention heatmaps, we first tokenized the generated reasoning and then computed attention values within the LLMs. These methods provide insights into the areas of focus in the MLLMs that lead to errors or failures in reasoning.

<sup>1</sup><https://huggingface.co/openai/clip-vit-large-patch14-336>

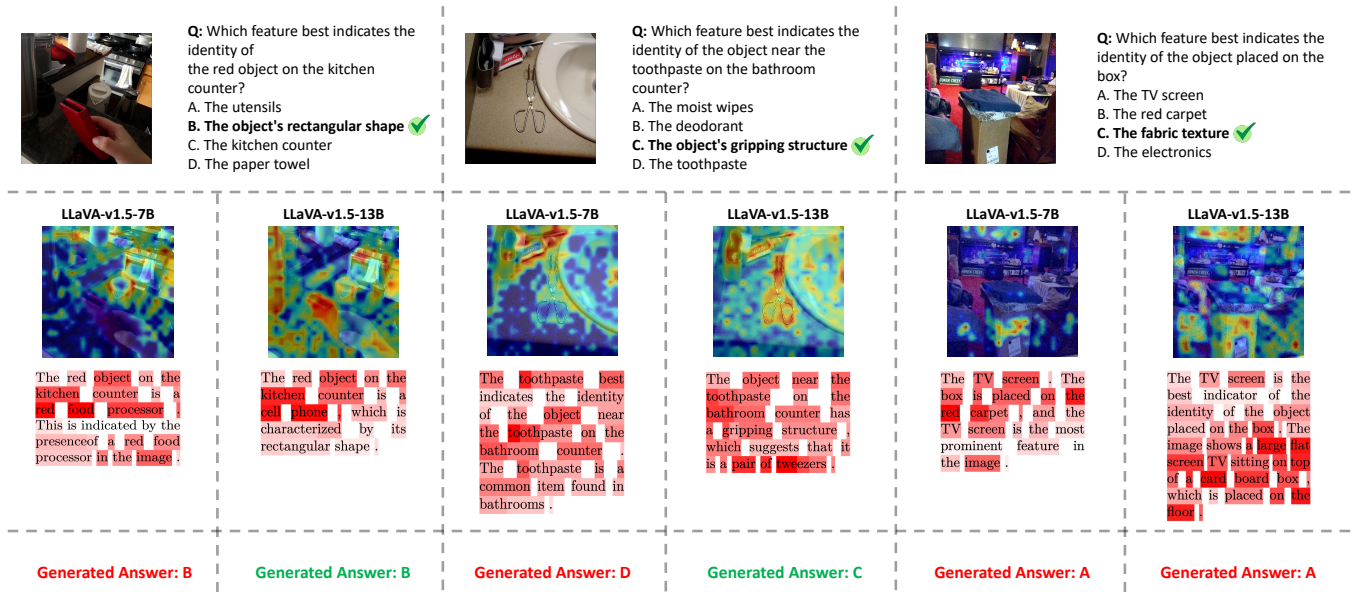


Figure 6: GradCAM Visualization and Text Attention Heatmap of MM-SpuBench on LLaVA 7B and 13B. The anchor objects in the three images are: a cellphone case, tweezers, and a full-sized towel.

Table 6: Text Prompts of Tested Prompt Methods

Strategy	Prompt
Guiding	"You need to describe the image first. Pay attention to the details that confirm your answer. Be mindful of the unrelated attributes in the image. Finally, end your answer with one letter."
No Bias	"Ensure that your answer is not affected by unimportant co-occurrence and spurious attributes. End your response with a one-letter answer."
Explain	"To answer the question, you need to explain why a certain option identifies the type of the object in the image. Finally, end your response with one one-letter answer."

**Table 7: Zero-shot results of different open-source MLLMs on MM-SpUBENCH with varying prompting methods. All numbers are percentage accuracies. Green color indicates higher accuracy, and red color indicates lower accuracy.**

Model	Prompt	BG	TN	CO	RS	Col.	Ori.	LS	PA	Sha.	Average
InternVL3-8B [90]	Vanilla	74.48	70.87	78.01	58.87	60.42	73.79	70.67	68.00	67.33	71.92
	Guiding	78.83	75.97	81.28	59.68	63.19	72.82	78.67	67.00	67.33	75.46
	No Bias	77.94	73.98	80.37	63.71	62.85	73.79	70.67	69.00	71.07	74.96
	Explain	75.05	71.54	78.14	60.48	61.46	74.76	76.00	67.00	69.33	72.67
InternVL3-14B [90]	Vanilla	81.55	80.51	82.85	64.92	66.32	75.73	80.00	69.00	64.09	77.92
	Guiding	78.35	77.19	79.58	60.48	61.46	73.79	76.00	68.00	64.34	74.88
	No Bias	83.44	82.39	85.08	65.32	66.67	77.67	82.67	73.00	66.08	79.75
	Explain	80.61	79.62	82.59	62.10	63.89	75.73	78.67	67.00	63.84	76.96
InternVL3-38B [90]	Vanilla	86.11	83.28	88.22	73.79	70.14	85.44	81.33	76.00	74.56	83.04
	Guiding	85.90	83.94	88.87	69.76	66.32	86.41	78.67	74.00	74.06	82.62
	No Bias	86.37	83.94	88.22	74.60	70.14	86.41	81.33	76.00	74.06	83.29
	Explain	86.06	83.94	87.43	73.39	69.44	86.41	80.00	74.00	75.06	82.96
Llama-3.2-VI-11B [46]	Vanilla	74.58	73.53	76.57	59.27	62.85	68.93	74.67	63.00	61.35	71.71
	Guiding	76.21	74.86	78.53	59.68	63.89	73.79	77.33	66.00	57.11	72.92
	No Bias	76.73	74.53	76.57	57.26	63.54	74.76	78.67	64.00	59.85	72.79
	Explain	77.73	74.53	79.71	60.89	64.24	79.61	78.67	69.00	61.85	74.25
LLaVA-v1.5-7B [39]	Vanilla	41.19	41.31	39.53	33.47	34.38	40.78	38.67	38.00	35.16	39.54
	Guiding	41.25	41.31	39.66	33.87	34.03	39.81	40.00	38.00	35.66	39.62
	No Bias	40.04	40.31	37.43	34.27	34.03	38.83	40.00	35.00	33.92	38.38
	Explain	41.51	40.86	39.40	35.08	35.07	40.78	40.00	37.00	34.91	39.67
LLaVA-v1.5-13B [39]	Vanilla	63.31	62.57	63.48	39.52	46.18	55.34	56.00	50.00	47.63	59.08
	Guiding	59.75	57.25	59.95	39.52	45.14	49.51	50.67	52.00	45.64	55.71
	No Bias	63.89	61.46	64.40	38.31	47.57	55.34	53.33	54.00	46.63	59.25
	Explain	64.10	61.79	64.27	41.94	48.26	59.22	53.33	53.00	47.63	59.75
LLaVA-v1.6-mis-7B [39]	Vanilla	40.88	41.20	41.36	34.27	39.24	39.81	40.00	41.00	34.41	39.96
	Guiding	40.57	38.65	41.62	34.68	36.46	35.92	45.33	33.00	33.17	39.00
	No Bias	40.15	39.87	40.05	34.27	41.32	41.75	41.33	40.00	33.92	39.33
	Explain	34.17	34.00	35.73	33.47	36.81	33.01	36.00	31.00	27.18	33.83
LLaVA-v1.6-vic-13B [39]	Vanilla	21.75	20.16	22.77	15.73	26.39	21.36	18.67	17.00	13.97	20.75
	Guiding	25.31	24.36	25.52	22.98	23.96	25.24	22.67	26.00	21.95	24.67
	No Bias	52.46	52.60	54.32	41.94	46.88	43.69	52.00	41.00	41.40	50.58
	Explain	50.68	51.27	52.49	42.74	46.88	43.69	49.33	41.00	40.90	49.29
Qwen2-VL-7B [6]	Vanilla	73.95	69.44	74.21	52.02	56.25	69.90	73.33	61.00	55.36	69.04
	Guiding	73.27	68.44	73.95	53.23	56.60	71.84	73.33	63.00	61.35	69.17
	No Bias	71.59	67.55	72.25	48.39	52.78	68.93	68.00	64.00	56.61	67.04
	Explain	75.58	69.88	76.44	54.03	59.03	71.84	73.33	63.00	62.84	71.12
Qwen2.5-VL-7B [7]	Vanilla	71.59	67.55	73.43	53.63	58.33	73.79	74.67	56.00	61.85	68.38
	Guiding	63.31	58.47	64.92	50.00	52.08	54.37	72.00	53.00	56.11	60.42
	No Bias	71.59	67.88	72.51	56.45	59.72	70.87	77.33	59.00	64.59	68.79
	Explain	64.62	60.13	65.84	50.40	51.74	63.11	73.33	55.00	54.36	61.54

### Prompt template for QA Generation

#### System Message

You are a helpful assistant that analyze images.

#### User Prompt

I will give you an image: <image>

true label: ... misclassified labels: ...

Spurious correlations are brittle associations learned by the models between non-essential spurious attributes of inputs and the corresponding core learning attributes in the training dataset.

Based on the provided information 1. Figure out what kind of spurious correlations is performing in the given image. 2. Based on the true label and the image, generate what are the core attributes of this true object label. Based on the misclassified labels and the image, generate what are the spurious attributes that are causing the misclassification. 3. Generate a multiple choice question based on the analysis to test the capability of a model whether it can identify the true label based on the spurious attributes. Among the choices, there should be only one correct answer related to the core attributes. Make the other choices as misleading as possible so that the model may fail on it. 4. Do not provide the true label or the core attributes of the main object in the question. Only use its visible spurious attributes or its spatial position in the image to refer to the object.

The max words for each attribute is {max\_words\_per\_attribute}.

The max number of core attributes is {num\_core\_attributes}.

The max number of spurious attributes is {num\_spurious\_attributes}.

For the generated multiple choice questions, the number of correct options is 1, and the number of wrong options is {num\_wrong\_options}.

You should only respond in the format as described below:

#### Response Format

*Explanation:* The explanation of the attributes.

*Core Attributes:* The core attributes of the main object, must be visible in the image.

*Spurious Attributes:* The spurious attributes in the image.

*Spurious Correlation Type:* Should be from the 9 possible categories: Background; Texture and Noise; Co-occurring Objects; Relative Size; Colorization; Orientation; Lighting and Shadows; Perspective and Angle; Shape. Two at most.

*Questions:* The question to ask about the image.

*Choices:* The choices for the question, indexed by a single letter.

*Answer:* The index of the correct answer, as a single letter.

Figure 7: Prompt template for system message and response format for the QA generation with GPT-4V.

### Prompt template for zero-shot evaluation

#### System Message

You are a helpful assistant that can answer question for an image. I will provide you 4 options.

#### User Prompt

<image>

Here is the question: ...

Here are the choices:

A. ...

B. ...

C. ...

D. ...

#### Response Format

*Choice:* A single character from A, B, C, D.

Figure 8: Prompt template for system message and response format for the zero-shot evaluation on open-sourced models.

Prompt template for zero-shot evaluation

**System Message**

You are a helpful assistant that can answer question for an image. I will provide you 4 options.

**User Prompt**

<image>

Here is the question: ...

Here are the choices:

A. ...

B. ...

C. ...

D. ...

**Response Format**

*Explanation:* Explanation text in one sentence.

*Choice:* A single character from A, B, C, D.

Figure 9: Prompt template for system message and response format for the zero-shot evaluation on proprietary models.

Prompt template for chain-of-thought evaluation

**System Message**

You are a helpful assistant that can answer question based on the image. Spurious correlations are brittle associations learned between non-essential spurious attributes of inputs and the corresponding core learning attributes. I will first provide you with the potential spurious correlation existing in the image. Then I will ask you a question with 4 options. Think step by step and then choose the best answer from the choices.

**Step 1**

The type of spurious correlation occurs in the images are <type1> and <type2>.

<type1> occurs when the model .... One example is ...

<type1> occurs when the model .... One example is ...

**Step 2**

<image>

Here is the question: ...

Here are the choices:

A. ...

B. ...

C. ...

D. ...

**Response Format**

*Explanation:* Explanation text in one sentence.

*Choice:* A single character from A, B, C, D.

Figure 10: Prompt template for system message and response format for the chain-of-thought evaluation on proprietary models.

**Assistant Prompt template for CGL calculation****System Message**

You are a helpful assistant that can answer question based on the image.

**User Prompt**

<image>

What's the distinguishing attribute of the object? What is <object\_literal>? Answer in the format: I see [object\_attribute], so the mentioned object is of type: [object\_class].

**Assistant**

I see <attribute\_text>, so the mentioned object is of type: <start\_of\_generation>

**User Prompt template for CGL calculation****System Message**

You are a helpful assistant that can answer question based on the image.

**User Prompt**

<image>

This image shows <attribute\_text>. What is <object\_literal>? Answer in this format: This is an object of type: <object\_class>."

**Assistant**

This is an object of type: <start\_of\_generation>

**Figure 11: Prompt template for the CGL evaluation on open-sourced models.**

**Prompt template for reasoning in visualization****System Message**

You are a helpful assistant that can answer questions based on the image. Provide a concise answer and explain your reasoning clearly.

**User Prompt**

<image>

Here is the question: ...

Here are the choices:

A. ...

B. ...

C. ...

D. ...

**Response Format**

*Explanation:* Provide a detailed explanation of your reasoning for selecting the choice.

*Choice:* A single character from A, B, C, D.

**Figure 12: Prompt template for reasoning in Grad-CAM visualization on LLaVA.**

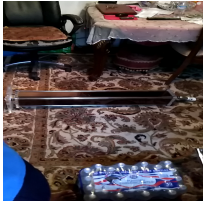
Image	Question	Choices	Answer	Type
	Which feature best indicates the identity of the object <b>held in hand on the countertop</b> ?	A. The countertop B. The lighting C. The metallic parts D. The multiple tools	D	Texture and Noise Shape
	Which feature best indicates the identity of the object that is <b>lying horizontally on the bathroom sink</b> ?	A. The object's control panel B. The bathroom mirror C. The toothbrushes D. The soap dispenser	A	Background Orientation
	Which feature best indicates the identity of the object that is <b>lying horizontally on the floor</b> ?	A. Office chair B. Water bottles C. Table D. Light bulb socket	D	Orientation Co-occurring Objects
	Which feature best indicates the identity of the <b>small cylindrical object next to the small bottle</b> ?	A. Its small size B. Its cylindrical shape C. The lace tablecloth D. The nearby bottle	B	Co-occurring Objects Relative Size

Table 8: More Data instances in MM-SPUBENCH. Images are cropped and resized to fit in the table. **Red** denotes the spurious attributes and **green** denotes the core attributes.

Image	Question	Choices	Answer	Type
	Which feature best indicates the identity of the object <b>being held</b> ?	<p>A. The glitter bottle</p> <p>B. The object's circular shape</p> <p>C. The shadow</p> <p>D. The surface texture</p>	B	Background Lighting and Shadows
	Which feature best indicates the identity of the object that is upside down <b>with two sticks on top</b> ?	<p>A. Circular shapes</p> <p>B. The shark-like form</p> <p>C. The cinnamon sticks</p> <p>D. The curved handle</p>	D	Orientation Shape
	Which feature best indicates the identity of the object with a <b>distorted reflection</b> ?	<p>A. The bulb shape</p> <p>B. The background buildings</p> <p>C. The outdoor setting</p> <p>D. The lightning</p>	A	Background Perspective and Angle
	Which feature best indicates the identity of the animal <b>with black and white patterns</b> ?	<p>A. Small size</p> <p>B. Dog-like head shape</p> <p>C. Black and white pattern</p> <p>D. Elongated body</p>	B	Colorization Orientation
	Which feature best indicates the identity of the <b>coiled object</b> in the drawing?	<p>A. The patterns on the object</p> <p>B. The serpentine body</p> <p>C. The outline drawing</p> <p>D. The coiled shape</p>	B	Shape Texture and Noise

**Table 9: More data instances in MM-SpuBENCH. Images are cropped and resized to fit in the table. Red denotes the spurious attributes and green denotes the core attributes.**